# CHARLES UNIVERSITY

FACULTY OF PHARMACY IN HRADEC KRÁLOVÉ

DPT. OF PHARMACEUTICAL CHEMISTRY AND PHARMACEUTICAL ANALYSIS


# "Design, synthesis and evaluation of heterocyclic compounds with potential antimicrobial activity VI"

Diploma Thesis

Nechirwan Abdalrahman

**Supervisor:** Assoc. Prof. PharmDr. Jan Zitko, Ph.D.

**Consultant:** Mgr. Vinod Sukanth Kumar Pallabothula

Hradec Králové 2023

# ACKNOWLEDGEMENT

I would like to express my heartfelt gratitude to Assoc. PharmDr. Jan Zitko for his exceptional patience, unwavering encouragement, and profound knowledge that have continuously fueled my passion and dedication, then my sincere thanks to Mgr. Vinod Pallabothula for his invaluable help and continuous support.

Furthermore, I wish to express my appreciation to the entire department for their support and collaborative spirit.

*The study was supported by the Ministry of Education, Youth and Sports of the Czech Republic (SVV 260 666) and Grant Agency of Charles University, project GA UK No. 349721. Supported by „The project National Institute of virology and bacteriology (Programme EXCELES, ID Project No. LX22NPO5103) - Funded by the European Union - Next Generation EU.“*

# Declaration

“I declare that the thesis is my original author's work, which has been consisted solely by myself (under the guidance of Assoc. Prof. PharmDr. Jan Zitko, Ph.D.). All the literature and resources from which I got information were cited in the list of used literature. The work has not been used to get another or the same title.”

Nechirwan Abdalrahman

Hradec Králové, August 2023

# Contents

# 1. List of Abbreviations

| | |
|---|---|
| aaRS | aminoacyl tRNA synthetase |
| AMP-aa | aminoacyl-adenylate |
| ARB | antimicrobial-resistant bacteria |
| DR-TB | drug-resistant tuberculosis |
| EMB | ethambutol |
| HGT | horizontal gene transfer |
| HIV | human immunodeficiency virus |
| IleRS | isoleucyl-tRNA synthetase |
| INH | Isoniazid |
| MDR | multidrug resistance / resistant |
| MDR-TB | multidrug-resistant tuberculosis |
| MoA | mechanism of action |
| *Mtb* | *Mycobacterium tuberculosis* |
| MW | microwave |
| POA | pyrazinoic acid |
| pre-XDR-TB | pre-extensively resistant tuberculosis |
| ProRS | prolyl-tRNA synthetase |
| PZA | pyrazinamide |
| RIF | rifampicin |
| RpsA | ribosomal protein S1 |
| RR-TB | rifampicin-resistant tuberculosis |
| TB | tuberculosis |
| WHO | World Health Organization |
| XDR-TB | extensively resistant tuberculosis |

# 2. Abstract (In Czech)

Univerzita Karlova

Farmaceutická fakulta v Hradci Králové

Katedra farmaceutické chemie a farmaceutické analýzy

**Autor:** Nechirwan Abdalrahman

**Školitel**: doc. PharmDr. Jan Zitko, Ph.D.

**Název:** Návrh, syntéza a hodnocení heterocyklických sloučenin s potenciální antimikrobní aktivitou VI

Navzdory existenci dobře zavedených léčebných režimů je tuberkulóza (TBC) nadále hlavní příčinou úmrtí jediného mikroorganismu, jak uvádí WHO. Jedním z důvodů selhání léčby při úplné eradikaci této infekce je léková rezistence.

Nové 3-(fenylureido)pyrazin-2-karboxamidové deriváty, viz obrázek níže, byly syntetizovány reakcí 3-chlorpyrazin-2-karboxamidu s amoniakem za vzniku 3-aminopyrazin-2-karboxamidu jako meziproduktového stavebního bloku, následovanou reakcí s různé substituované fenylisokyanáty za použití mikrovlnného reaktoru.

U syntetizovaných sloučenin byla hodnocena in vitro aktivita proti různým mykobakteriálním kmenům, přičemž nejaktivnější z nich vykazovaly střední až nízké aktivity; 4-terciární butyl (MIC 62,5 µg/ml), 4-NO2 (MIC 62,5 µg/ml), 4-brom (MIC 250 µg/ml), 4-Cl (MIC 250 µg/ml), 2-F (MIC 250 ug/ml) a nesubstituované (MIC 500 ug/ml).

Jako doplňková studie in silico byly syntetizované sloučeniny a některé další virtuálně syntetizované sloučeniny studovány na mykobakteriální inhibici ProRS jako předpokládaný cíl pro sloučeniny uvedené v názvu.

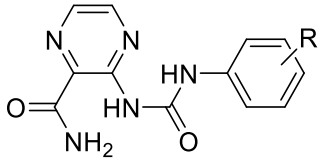


**R:** H, 2-$CH_3$, 3- $CH_3$, 4- $CH_3$, 2-Cl, 4-Cl, 2-$OCH_3$, 3- $OCH_3$, 4- $OCH_3$, 4-*t*-Bu, 2-F, 3-F, 4-F, 4-$NO_2$, 2-Br, 3-Br, and 4-Br.

**Obrázek:** Chemické struktury titulních sloučenin.

# 3. Abstract (In English)

Charles University

Faculty of Pharmacy in Hradec Králové

Department of Pharmaceutical Chemistry and Pharmaceutical Analysis

**Author:** Nechirwan Abdalrahman

**Supervisor:** Assoc. Prof. PharmDr. Jan Zitko, Ph.D.

**Title:** Design, synthesis, and evaluation of heterocyclic compounds with potential antimicrobial activity VI

Despite the existence of a well-established treatment regimens, tuberculosis (TB) continues to be the most leading cause of death by a single microorganism, as reported by WHO. One of the reasons behind treatment failure in completely eradicating this infection is drug resistance.

Novel 3-(phenylureido)pyrazine-2-carboxamide derivatives, refer to figure below, were synthesized by reacting 3-chloropyrazine-2-carboxamide with ammonia to produce 3-aminopyrazine-2-carboxamide as an intermediate building block, followed by reacting with various substituted phenyl isocyanates using a microwave reactor.

The synthesized compounds were evaluated for *in vitro* activity against various mycobacterial strains, where most active ones among them showed moderate to low activities; 4-tertiary butyl (MIC 62.5 µg/mL), 4-$NO_2$ (MIC 62.5 µg/mL), 4-Bromo (MIC 250 µg/mL), 4-Cl (MIC 250 µg/mL), 2-F (MIC 250 µg/mL), and non-substituted (MIC 500 µg/mL).

As a complementary study *in silico*, the synthesized compounds and some other virtually synthesized were studied for mycobacterial ProRS inhibition as a supposed target for the title compounds.

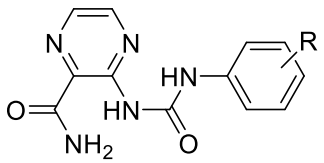


**R:** H, 2-$CH_3$, 3- $CH_3$, 4- $CH_3$, 2-Cl, 4-Cl, 2-$OCH_3$, 3- $OCH_3$, 4- $OCH_3$, 4-*t*-Bu, 2-F, 3-F, 4-F, 4-$NO_2$, 2-Br, 3-Br, and 4-Br.

**Figure:** The chemical structures of title compounds.

# 4. Aim

The main aim of the research is to synthesize novel 3-(phenylureido)pyrazine-2-carboxamide derivatives as antimicrobial agents. The design is based on previously described 3-benzamidopyrazine-2-carboxamide analogues, which possessed significant *in vitro* antimycobacterial activity and were computationally predicted to bind to a homology model of mycobacterial prolyl-tRNA synthetase (Figure 1) [1].

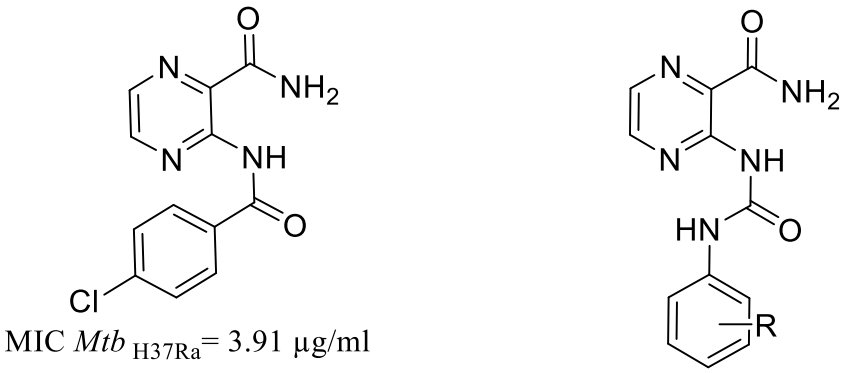


**R:** H, 2-$CH_3$, 3-$CH_3$, 4-$CH_3$, 2-Cl, 4-Cl, 2-$OCH_3$, 3-$OCH_3$, 4-$OCH_3$, 4-*t*-Bu, 2-F, 3-F, 4-F, 4-$NO_2$, 2-Br, 3-Br, and 4-Br.

**Figure 1: Left:** Published 3-(4-chlorobenzamido)pyrazine-2-carboxamide [1].

**Right:** General structure of our compounds.

# 5. Introduction

The constant requirement for novel antimicrobial agents is a persistent challenge to overcome newly acquired resistance against conventional antimicrobials [2].

The number of deaths caused by antimicrobial resistance is estimated by 1.27 million annually [3].

Regarding *Mycobacterium tuberculosis* (*Mtb*), the focus of our study, as it is known, 6.4 million cases in 2021 were reported with tuberculosis (TB), and death estimation in 2021, was 1.4 million. While drastic decrease can be seen during 2020 and 2021, which was because of covid-19 pandemic basically (Figure 2) [4].

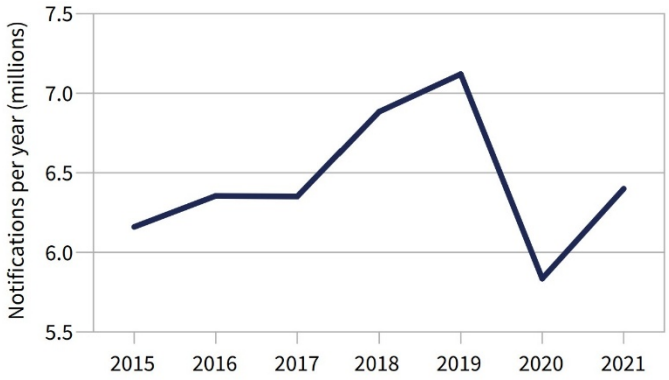


**Figure 2:** Global case reporting of TB from 2015–2021. Taken from [4].

Thus, the focus has been given to synthesize new antituberculosis compounds with newer and more efficient mechanism of action (MoA), preferably different to the MoA of currently used antitubercular.

## 5.1. Mycobacteria

Is an elongated, rod-like shape and thin bacterium, measuring 0.5µm by 0.3µm with lacking spore-forming capability. Mostly neutral on Gram's staining. And it grows parallelly as a group named cords. It is a member of the family *Mycobacteriaceae* and the order *Actinomycetales* [5] [6].

Being a pathogenic species within *Mtb* complex (the complex comprising eight subgroups) and stands out as the most common and leading cause of human disease to a considerable extent.

The *Mtb* complex comprises some zoonotic members, such as *M. bovis* (which is characteristically resistant to pyrazinamide), *M. caprae*.

*Mtb* can be classified as acid-fast bacilli due to its abundant mycolic acids, lipid, and long-chain cross-linked fatty acid content.

Lipids (e.g., mycolic acids) within the cell wall are connected to underlying arabinogalactan and peptidoglycan, leading to extremely limited permeability. This, in turn, decreases the efficacy of most antimicrobial compounds [7]

Furthermore, another component of the mycobacterial cell wall, known as lipoarabinomannan, contributes to the interaction between the pathogen and the host, and aids the persistence of *Mtb* within macrophages [6].

## 5.2. Tuberculosis

Tuberculosis is an infectious disease caused by the bacillus *Mycobacterium tuberculosis*, ranking among the primary contributors to global mortality (Figure 3), and most causing death by a single microorganism [4].

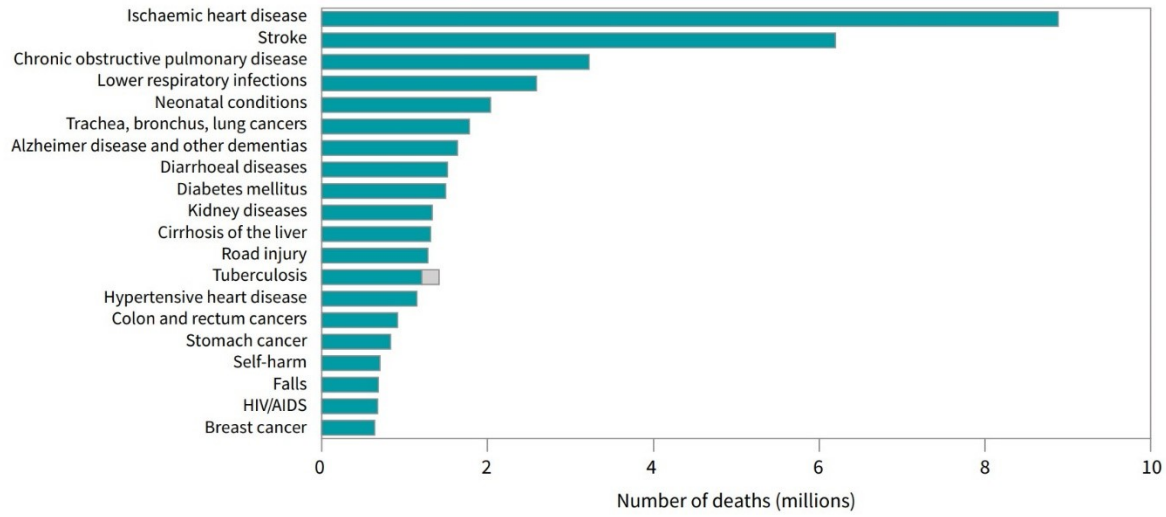


**Figure 3:** The leading causes of death in 2019. Taken from [4].

It is also an airborne disease (e.g., through coughing), and about one-fourth of the population is assumed to get latent tuberculosis infection [8].

The incubation time of *Mtb* to became a disease from the infection is from months to two years [9].

The lungs are the most affected organ by TB in young people, with a higher likelihood of infection compared to other organs [10] [4].

Among the most risk factors that cause *Mtb* to be transmitted, are:

- Organism's number that spread.
- Organism's concentration.
- Exposure time to infected air.
- Patient's immunity status.

Also, there are many risk factors that make the patient more prone to get active *Mtb* infection:

- HIV infection
- Drug abuse
- Diabetes mellitus
- Cancer
- Genetic factor
- And others.…[6]

## 5.3. Diagnosis of Tuberculosis

About 6.4 million case were diagnosed with TB in 2021, while the incidence target to be achieved in 2035 via End TB strategy by WHO (for prevention, care, and control of TB from 2015 afterward) is 10 cases per 100,000 of population [11].

Thus, early, correct, and precise diagnosis of TB is a fundamental factor for controlling the pandemic [12].

Tuberculosis's symptoms are usually fever, adynamia, anorexia, weight loss, night sweats and symptoms associated with the area being affected [11].

The most used tests that used to diagnose TB include:

- Bacteriological, which is very useful for detection and diagnosis of active tuberculosis.[13].
- The Molecular testing that can be used is The Xpert MTB/RIF assay, which depends on nucleic acid detection of MB-DNA [11].
- Another important tool for the detection of respiratory diseases is radiology, which includes X-Ray and CT scans, which provide information about the manifestation and extent of the disease and the course of treatment [14].
- Histopathological test is another crucial method used to diagnose *Mtb*, which provides information about pulmonary and extrapulmonary forms of the disease.

## 5.4. Bacterial Resistance

Antimicrobial resistant bacteria (ARB) are a burdensome, continuous, and risky problem for people's health worldwide, which may lead to longer hospitalization, increased costs, and mortality rate [15].

Incorrect usage and frequent administration of antimicrobials are primary factors leading to development of microbial resistance. Consequently, it leads to higher incidence of multidrug resistance (MDR), and vice versa [16], [17].

Substantially, the mode of bacterial resistance to antibiotics can be through or because of structural and functional features, which may lead to drug resistance through reducing of drug accumulation inside the bacterium or through the inactivation of the drug [18] [19].

Although, resistance by genes can be obtained through mutation in chromosomal genes or in horizontal gene transfer (HGT), whereas mutation in chromosomes takes place in DNA level during DNA replication and causes DNA-modification [20].

But for horizontal gene transfer (HGT), mutation happens through its transferring or acquiring of genetic materials via other microbes. HGT includes; transposons, plasmids, and integrons, mostly [21].

## 5.5. Mycobacterial Resistance

Antitubercular resistance is a major cause of TB treatment failure and increased mortality rate consequently [22].

Genetic mutations and other contributors beside selective environmental factors are among the mechanisms to develop resistance by *Mtb*. Environmental factors may lead to genetic mutations which can decrease effectiveness of antitubercular drugs and give the *Mtb* an ability to survive in extreme environmental condition [23].

Drug resistant tuberculosis (DR-TB) is classified into five subcategories, which are: Isoniazid-resistant TB, rifampicin resistant TB (RR-TB), multidrug resistant TB (MDR-TB), extensively resistant TB (XDR-TB and pre-extensively resistant TB (pre-XDR-TB).

XDR-TB is a resistance against rifampicin, all fluoroquinolones, and either bedaquiline or linezolid, while pre-XDR-TB has resistance to rifampicin and all fluoroquinolones [24].

On a global basis, in 2021, 71% (2.4/3.4 million) of TB cases were tested bacteriologically to detect DR-TB. For MDR-TB, 141,953 cases, and for pre-XDR-TB and XDR-TB, 25,038 cases were resistant (Figure 4) [4].

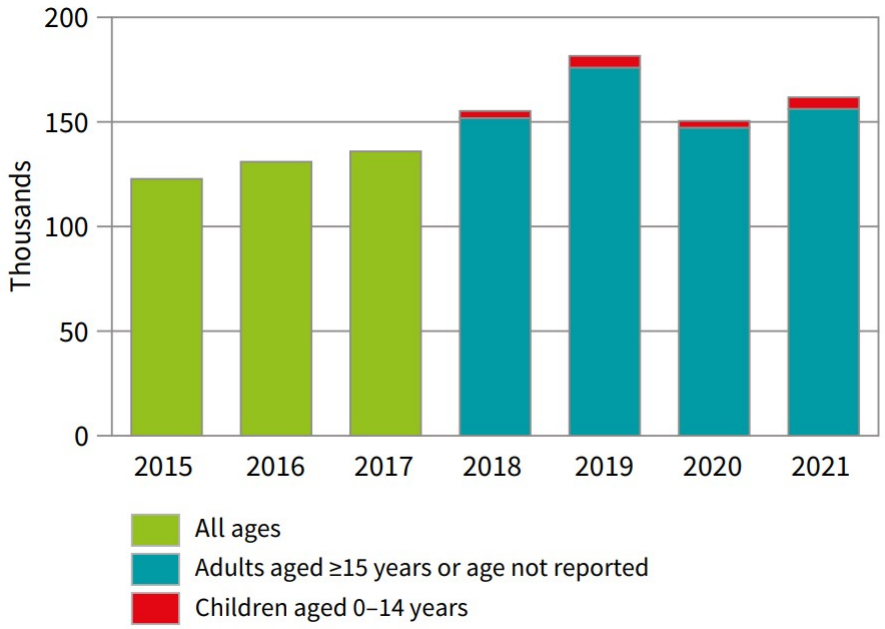


**Figure 4:** Depicting the number of reported individuals to have been registered on treatment for MDR/RR-TB, from 2015-2021. Taken from [4].

Knowing the mechanism of resistance is a crucial step to design and develop new antimicrobials. Consequently, reducing MDR [25].

### 5.5.1. Pyrazinamide resistance

Pyrazinamide stands as one of the most effective treatment options for both drug-susceptible and MDR-TB, and for its impact on shortening the course of the treatment [26] [27].

Pyrazinamide should be converted to its active form inside the mycobacterium which is pyrazinoic acid (POA) by enzyme; nicotinamidase/pyrazinamidase which is encoded by a *pncA* gene. Mutation of this gene is a major cause of PZA resistance in TB [27].

Other mechanisms of resistance to PZA include ribosomal protein S1(RpsA, Rv1630) that has a crucial role in trans-translation [28], or mutation occurring in *panD* gene, which is responsible for encoding aspartate decarboxylase[27].

## 5.6. Current Treatment of Tuberculosis

First-line treatment regimen of tuberculosis (their structures are shown in Figure 5 below) consists of:

- isoniazid (INH)
- rifampin (RIF)
- pyrazinamide (PZA)
- ethambutol (EMB) [5].

Isoniazid and rifampicin should be given for six months, and pyrazinamide and ethambutol for the first two months of the six-month treatment regimen [29].

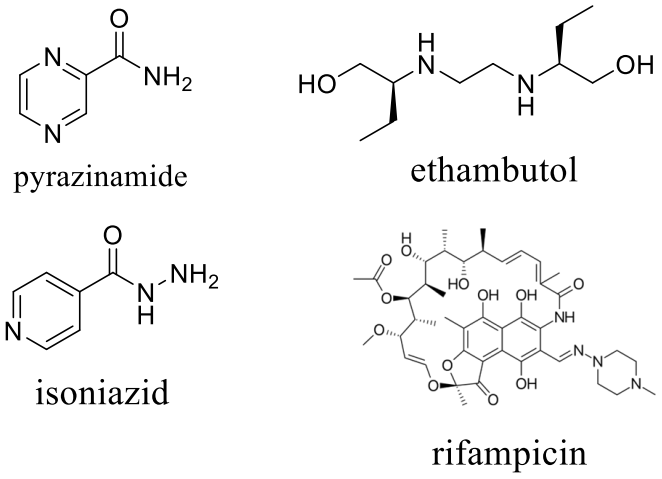


**Figure 5:** Chemical structures of first line antimycobacterial drugs.

Whereas a recommendation by WHO in 2022, for treating drug-resistance tuberculosis, MDR/RR-TB and pre-XDR-TB, is using six-month regimen composed of bedaquiline, pretomanid, linezolid and moxifloxacin.

Also, another reprinted recommendation where no newer evidence available, includes nine-month regimen with the same drugs for MDR/RR-TB rather than 18-month, but with the exclusion of fluoroquinolones in case of resistance.

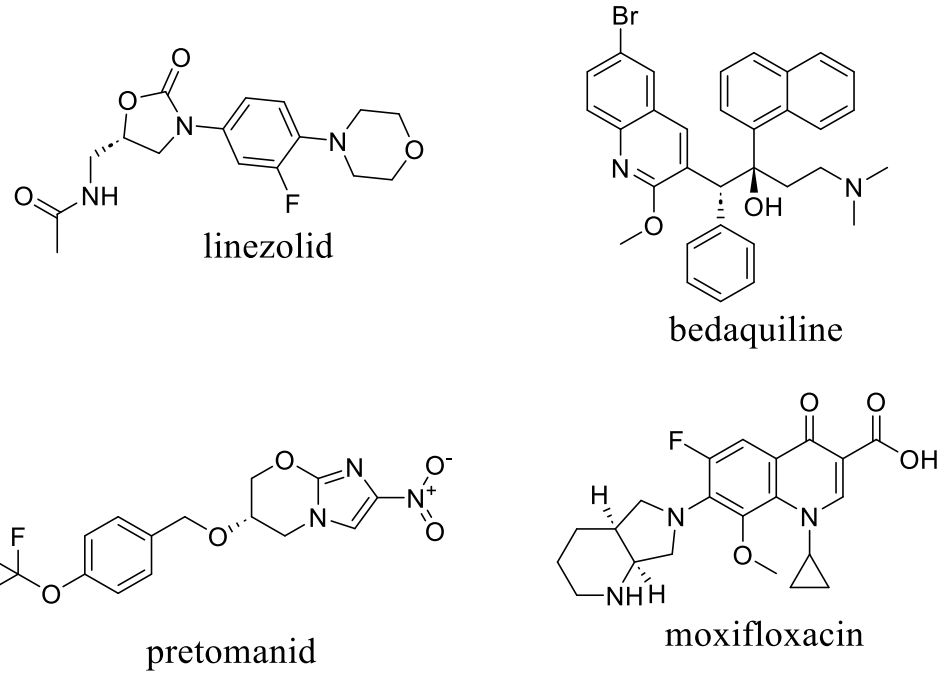


**Figure 6:** Chemical structures of antimycobacterial drugs for MDR/RR-TB and pre-XDR-TB.

For rifampicin-susceptible and isoniazid-resistant TB, six-month treatment together with rifampicin, ethambutol, pyrazinamide, and levofloxacin should be used [30].

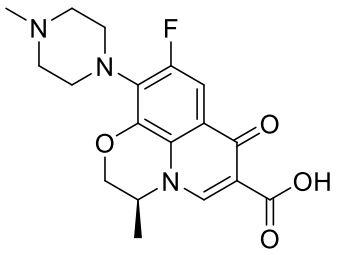


**Figure 7:** Chemical structure of levofloxacin.

## 5.7. Aminoacyl-tRNA synthetases as a new target and as our target

Aminoacyl-tRNA synthetases are a class of essential enzymes present in all eukaryotes, archaea, and bacteria [31], which have a crucial role in ligating amino acids to their cognate tRNA. The mechanism commences by forming an enzyme-bound aminoacyl-adenylate (AMP-aa). Subsequently, the amino acids are transferred to their corresponding tRNAs to form aminoacylated-tRNAs, and protein synthesis (figure 8) [32].

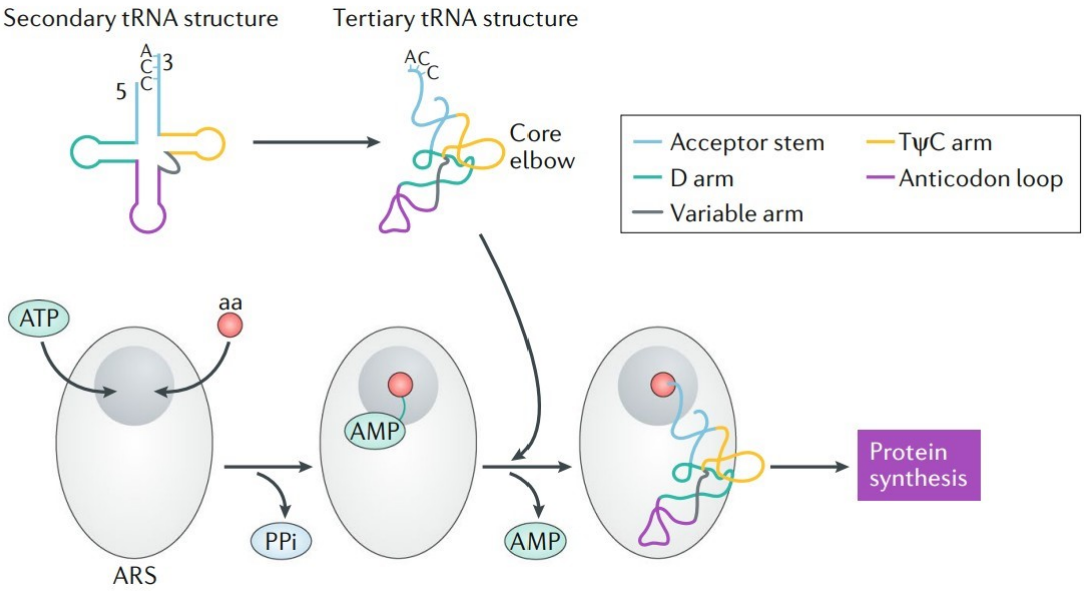


**Figure 8:** Catalytic reaction of aaRSs. Taken from [34].

It can causes precise gene translation by using cognate substrate recognition and stringent proofreading of non-cognate substrates [33]. Inhibition of aminoacyl-tRNA synthetase has been established as an important antimicrobial strategy with proven effectiveness, and there are three aminoacyl-tRNA synthetase inhibitors; mupirocin which can inhibit isoleucyl-tRNA synthetase (IleRS), monocarboxylic class, and clinically used as an antibacterial drug against methicillin-resistant staphylococcus aureus (MRSA) [35, 36], Tavaborole is an irreversible inhibitor of fungal leucyl-tRNA synthetase, and halofuginone which is non-competitive inhibitor of protozoal prolyl-tRNA synthetase (Figure 9)[1].

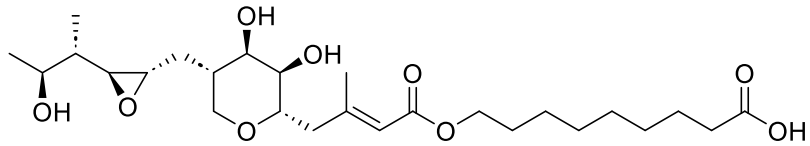


mupirocin

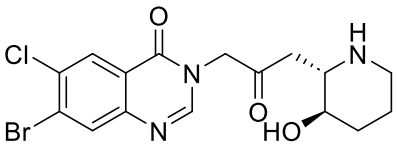


halofuginone

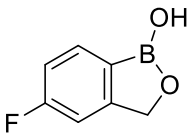


tavaborole

**Figure 9:** Chemical structures of aminoacyl-tRNA synthetase inhibitors; mupirocin, tavaborole, and halofuginone.

In a recently published article, novel compounds were introduced as a newer category of antimicrobial agents based on 3-aminopyrazinamide, which perform their mechanism of action through inhibition of mycobacterial prolyl-tRNA (mtProRS) synthetase. The ligand-protein interaction diagram of the best active compound with 4-chlorobenzoyl substitution is presented below (Figure 10) [1].

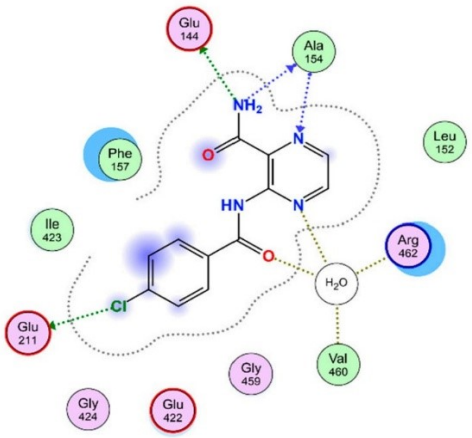


**Figure 10:** Ligand-protein interaction of 3-(4-chlorobenzamido)pyrazine-2-carboxamide.

Thus, our aim was to design novel compounds by substituting the amidic linker with urea-linker, and then to evaluate their activity.

# 6. Experimental part

## 6.1. General, laboratory equipment and instruments

All chemicals (unless stated otherwise) were purchased from Merck (Taufkirchen, Germany) and Flurochem (Hadfield, United Kingdom). The reaction progress and the purity of the final compounds were checked using Merck Silica 60 $F_{254}$ TLC plates (Merck, Darmstadt, Germany). Purification of synthesized compounds was performed on automated flash chromatograph puriFlash XS420+ (Interchim, Montluçon, France) using original columns (silica, 30 μm). The mixture of ethyl acetate and hexane was used as a mobile phase with elution gradient 0–100% ethyl acetate (EtOAc) to hexane (Hex.), and detection was performed by UV-VIS detector at a wavelength of 254nm and 280nm. NMR spectra were recorded on Varian VNMR S500 (Varian, Palo Alto, CA, USA) at 500 MHz for $^{1}H$ and 125 MHz for $^{13}C$ or using Jeol JNM-ECG600 at 600 MHz for $^{1}H$ and 151 MHz for $^{13}C$. The spectra were recorded in DMSO-$d_6$ at 40˚C to 60˚C temperature. The chemical shifts as δ values in ppm are indirectly referenced to tetramethylsilane (TMS) via the solvent signal. Nicolet 6700 spectrometer (Thermo Scientific, Waltham, MA, USA) was used to measure IR spectra using ATR-Ge method. The purity of the newly synthesized compounds was checked with chemical composition and was recorded by an elemental analysis performed on Vario MICRO cube Element Analyzer (Elementar Analysensysteme, Hanau, Germany) with values given as percentages. The purity of the newly synthesized compounds with fluorine was measured using a Shimadzu LC20 chromatograph (Shimadzu, Kyoto, Japan) coupled with a PDA detector (SPD-M20A) on the ZORBAX ECLIPSE XDB-C18 (3.0 × 50 mm, 1.8 μm, Agilent Technologies, U.S.A) column using an acetonitrile/water mobile phase mixture in gradient mode. Data were processed using LabSolutions software (v. 5.92, Shimadzu, Kyoto, Japan). The stock solution of each compound (1.0 mg/mL) was prepared by dissolving the appropriate amount in methanol. Working solutions were prepared by diluting the stock solutions with the acetonitrile/water mixture (1:1, *v*/*v*) to a concentration of 50 μg/mL. The PDA detector acquired spectra from 190 to 380nm, and a wavelength of 260nm was employed for purity evaluation. The melting points of the synthesized compounds were measured in an open capillary on Stuart SMP30 melting point apparatus (Bibby Scientific Limited, Staffordshire, UK) and are uncorrected.

## 6.2. Chemistry

### 6.2.1. Synthesis of the starting compound 3-chloropyrazine-2-carboxamide

A solution mixture of 2.9 mL of conc. hydrogen peroxide (30%) and 19.5 mL of water were taken in a 100 mL round-bottomed flask (R. B. F) and then alkalinized to pH 9.0 by using sodium hydroxide solution (8%) and heated to 50 ˚C. 10 mmol (1.5 g) of 3-chloropyrazine-2-carbonitrile (Fluorochem) was added to the heated mixture portion-wise over a period of 30 minutes. The whole mixture was stirred for another 2.5 hr. at 55 ˚C, meanwhile, the pH was checked periodically and adjusted to 9.0 by adding NaOH solution. Light, yellow-colored precipitate/crystals of the product formed during the reaction process. The reaction mixture was cooled in the fridge for further crystallization. The light-yellow crude product was filtered under *vacuo* and recrystallized from ethanol while activated charcoal was used to absorb the colored impurities.

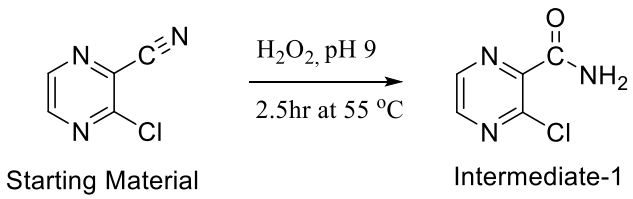


**Scheme 1:** Synthesis of 3-chloropyrazine-2-carboxamide by partial hydrolysis of the respective carbonitrile

**Comparision of starting material and intermediate-1( product) on TLC**

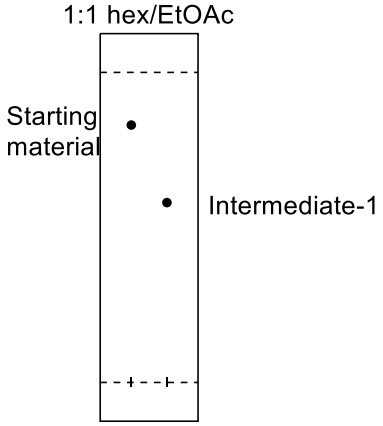

**3-chloropyrazine-2-carboxamide (intermediate-1)**

**Appearance:** White Crystals.

**Yield:** 65%.

**Melting point:** 187.0–188.8˚C (187.1–189.2˚C in previous article [37]).

**NMR:** $^{1}$H NMR (600 MHz, DMSO- $d_6$) δ 8.68 (d, $J$ = 2.5 Hz, 1H, PzH), 8.62 (d, $J$ = 2.5 Hz, 1H, PzH), 8.18 (s, 1H, CONH), 7.93 (s, 1H, CONH).

### 6.2.2. Chemical substitution of 3-chloropyrazine-2-carboxamide to synthesize 3-aminopyrazine-2-carboxamide

500 mg of 3-chloropyrazine-2-carboxamide was mixed with 3–4 mL of 7N $NH_3$ in anhydrous MeOH in a microwave tube. The reaction proceeded in a microwave reactor (MW) for 45 min (Power: 120 W, Temp.: 120 ˚C, Pressure limit: 120 psi). Once the reaction was completed, a white solid product was formed in the reaction mixture. The excess $NH_3$ in MeOH solvent was evaporated to dryness under *vacuo,* and the crude product was used for the next steps without further purification.

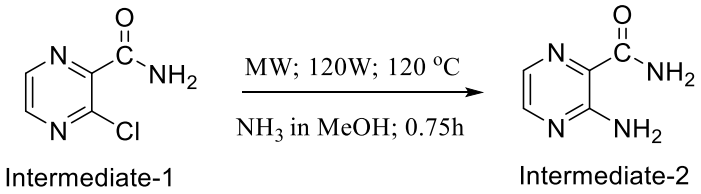


**Scheme 2:** Synthesis of 3-aminopyrazine-2-carboxamide

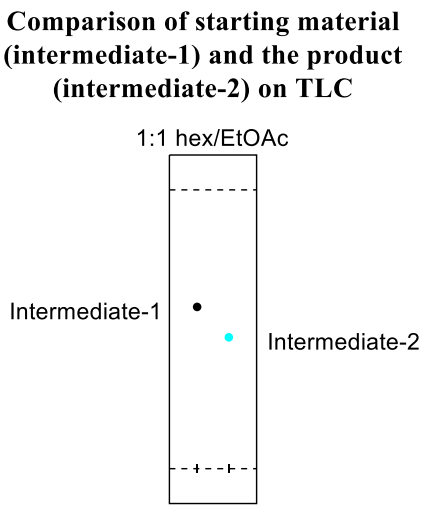

**3-aminopyrazine-2-carboxamide (intermediate-2)**

**Appearance:** White Solid.

**Yield:** 95%.

**Melting point:** 240.1–241.7 ˚C (238.4–239.4 from reference article) [38].

**NMR:** $^1$H NMR (600 MHz, DMSO-$d_6$) δ 8.18 (d, $J$ = 2.4 Hz, 1H, PzH), 8.06 (s, 1H, CONH), 7.80 (d, $J$ = 2.4 Hz, 1H, PzH), 7.58 (s, 1H, CONH), 3.33 (s, 2H, $NH_2$).

## 6.2.3. Synthesis of 3-(3-phenylureido)pyrazine-2-carboxamide derivatives

The 3-aminopyrazine-2-carboxamide (139 mg, 1 mmol) was reacted with different aryl-substituted isocyanates (2.2 mmol) in anhydrous acetonitrile (ACN) as a solvent (2 mL) in MW reactor using the following conditions (Power: 120 W, Temp.: 120 ˚C, Pressure limit: 120 psi). The solid precipitate was filtered under *vacuo* and washed with water to remove excess isocyanate reagent and followed by washing with 5 to 10mL of acetone and hexane followed by water. The crude solid precipitate was dissolved in small amounts of acetone under heating and precipitated using cold hexane and refrigerated. A white solid precipitate formed and was filtered under *vacuo,* then washed with cold acetone and hexane to remove any remaining impurities (as checked using TLC).

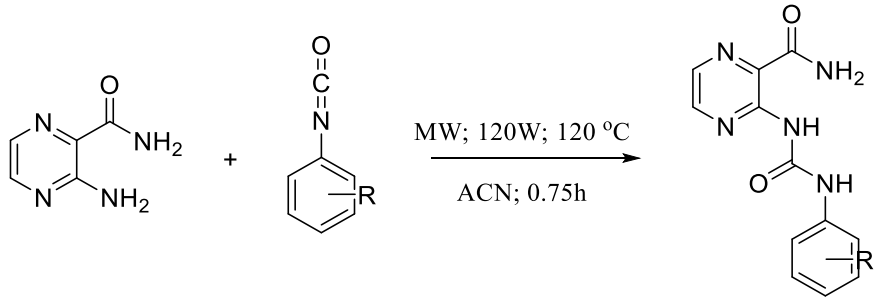


**Scheme 3:** Synthesis of 3-(3-phenylureido)pyrazine-2-carboxamide derivatives.

## 6.3. In silico simulations

### 6.3.1. Software

In silico calculations were performed in Molecular Operating Environment (MOE) 2022.02 (Chemical Computing Group Inc., Montreal, QC, Canada) under Amber10:EHT forcefield (if not otherwise stated). Structures were drawn in ChemDraw Professional, 20.0.0.41 (PerkinElmer Informatics, Inc., Waltham, MA, USA).

### 6.3.2. Preparation of ligands

57 differently substituted (on phenyl) derivatives of 3-(phenylureido)-pyrazine-2-carboxamides were drawn by ChemDraw, and then smile codes were generated to make a database.

After the database was ready, its preparation in MOE was done through "**WASH**", where the settings were set up like below (parameters not mentioned below were kept unchanged with default settings):

**Protonation**: Enumerate was chosen at pH 7, and the maximum number of generated protomers was limited to 10.

Using the above-mentioned application, the 3D structures of ligands were generated and minimized until RMS gradient 0.01 $kcal.mol^{-1}.Å^{-1}$. In some compounds, we were not happy with the acquired conformation (the urea linker conformation was distorted), so the second step was done to them via "**CONFORMATIONAL SEARCH**", where the settings were kept like:

**Method**: **LowModMD** was selected.

**Rejection Limit**: 100

**Iteration**: 10000

**RMS Gradient**: 0.005

**MM Iteration Limit**: 500

**RMSD Limit**: 0.25

**Energy Windows**: **7** and "**Separate strain energy by stereo class**" was ticked.

**Conformation Limit**: 10000

Thus, the compounds were ready for docking.

### 6.3.3. The receptor

Mycobacterial ProRS used in this project is a system created from overlay of mycobacterial prolyl-tRNA synthetase (mtProRS) homology model from the AlphaFold database (UniProt ID: P9WFT9) with experimental coordinates of proline and adenosine from ProRS of *Enterococcus faecalis* (pdb id: 2J3L). This model was optimized with further modifications, such as retaining the water molecule at the active site. The detailed process for the creation of the system was published before [1].

### 6.3.4. Molecular Docking

After the protein and the database of ligands were ready, through "DOCKING" in MOE, the docking was done where all settings kept as:

**Site**: Ligand atoms

**Ligand**: the database of our prepared ligands

**Conformations**: Rotate bonds

**Placement**: Triangle Matcher, scored by "**London dG**", 30 best poses retained

**Refinement:** "**Rigid receptor**", "GBVI/SA dG", 5 best poses retained.

**rigid and induced-fit**. were tried.

### 6.3.5. Analysis of docking results

After docking, a large database was generated, and selection of compounds with specific H-bonding through "PLIF" function in MOE, which were Ala154 HBD and Ala154 HBA, and to be more specific, then best scored poses (except for two to three of them) were selected.

## 6.4. Antimicrobial screening

**In vitro screening of antimycobacterial activity against *Mycobacterium tuberculosis* H37Ra, *M. smegmatis*, *M. aurum*, *M. avium*, *M. kansasii*.**

Microdilution assay (Microplate Alamar Blue Assay (MABA)) was performed as described in our earlier publications. The antimycobacterial assay was performed with fast-growing *Mycobacterium smegmatis* DSM 43465 (ATCC 607) and *M. aurum* DSM 43999 (ATCC 23366); non-tuberculous (atypical) mycobacteria, namely *Mycobacterium avium* DSM 44,156 (ATCC 25291) and *Mycobacterium kansasii* DSM 44,162 (ATCC 12478), from the German Collection of Microorganisms and Cell Cultures (Braunschweig, Germany) and with the avirulent strain of *Mycobacterium tuberculosis* H37Ra ITM-M006710 (ATCC 9431) from Belgian Coordinated Collections of Microorganisms (Antwerp, Belgium).

The technique used for activity determination was the microdilution broth method using 96-well microtitration plates. The culturing medium was Middlebrook 7H9 broth (Merck) with a defined pH of 6.6 ± 0.2 enriched with glycerol (Merck) and Middlebrook OADC growth supplement (Himedia, Mumbai, India) according to the manufacturer's instructions.

The mycobacterial strains were cultured on enriched Middlebrook 7H9 agar, and suspensions were prepared in enriched Middlebrook 7H9 broth. The final density was adjusted to value 1.0 according to McFarland scale and diluted in the ratio 1:20 (for fast-growing mycobacteria) or 1:10 (for *Mtb* H37Ra) with broth. The tested compounds were dissolved in dimethyl sulfoxide (DMSO) (Merck), then Middlebrook 7H9 broth was added to obtain a concentration of 2000 μg/mL. The standards used for activity determination were isoniazid (INH), rifampicin (RIF), and ciprofloxacin (CIP) (Merck).

The final concentrations were reached by binary dilution and the addition of mycobacterial suspension and were set as 500, 250, 125, 62.5, 31.25, 15.625, 7.81, 3.91, and 1.95 μg/mL. The final concentration of DMSO in any well did not exceed 2.5% (v/v) and did not affect the growth of mycobacteria. Positive (broth, DMSO, bacteria) and negative (broth, DMSO) growth controls were included. The plates were incubated in the dark at 37 °C without agitation.

The addition of 0.01% solution of resazurin sodium salt followed 48h of incubation for *M. smegmatis*, after 72 h of incubation for *M. aurum*, after 96 h of

incubation for *M. avium* and *M. kansasii*, and after 120 h of incubation for *Mtb* H37Ra, respectively.

The stain was prepared by dissolving resazurin sodium salt (Merck) in deionized water to get a 0.02% solution. Then, a 10% aqueous solution of Tween 80 (Merck) was prepared. Both liquids were mixed up making use of the same volumes and filtered through a 0.2 µm syringe membrane filter.

The microtitration panels were then incubated for a further 2.5 h for the determination of activity against *M. smegmatis*, 4 h for *M. aurum*, 5–6 h for *M. avium* and *M. kansasii*, and 18 h for *Mtb* H37Ra, respectively. The antimycobacterial activity was expressed as the minimum inhibitory concentration (MIC).

The MIC (in µg/mL) was determined based on stain color change (blue color—active; pink color—not active). The MIC values for standards are presented in the respective tables. All experiments were conducted in duplicate.

## 6.5. Monographs

**Compound 1:**

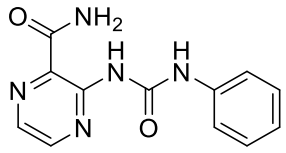

**Laboratory code:** H-VZN

**Chemical Name:** 3-(3-phenylureido)pyrazine-2-carboxamide

**Molecular weight:** 257.25 g/mol

**Yield:** 65 mg; 25.3%

**Appearance:** beige solid

**Melting point:** 224.3–226.2 °C

**$^{1}$H NMR** (600 MHz, DMSO-$d_6$): δ 11.30 (s, 1H, NHCO), 11.16 (s, 1H, NHCO), 8.60 (d, $J$ = 2.5 Hz, 1H, PzH), 8.49 (s, 1H, CONH), 8.34 (d, $J$ = 2.5 Hz, 1H, PzH), 8.10 (s, 1H, CONH), 7.64–7.57 (m, 2H, ArH), 7.39–7.29 (m, 2H, ArH), 7.08 (t, $J$ = 1.2 Hz, 1H, ArH)

**$^{13}$C NMR** (151 MHz, DMSO-$d_6$): δ 167.54, 150.71, 148.84, 143.98, 138.09, 135.39, 128.97, 128.69, 123.19, 119.57.

**Elemental analysis:**

Theoretical Values: C: 56.03%, H: 4.31%, N: 27.22%

Experimental values: C: 55.32%, H: 4.46%, N: 26.66%

**IR** (ATR-Ge, cm$^{-1}$): 3408, 3193, 1684 (C=O, CONH), 1655 (C=O, CONH), 1605, 1585, 1559, 1478 (Aromatic).

**Compound 2:**

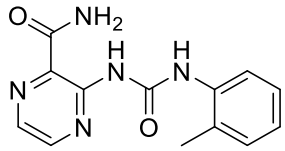

**Laboratory code:** 2-Me-VZN

**Chemical Name:** 3-(3-(*o*-tolyl)ureido)pyrazine-2-carboxamide

**Molecular weight:** 271.28 g/mol

**Yield:** 72 mg; 26.4%

**Appearance:** beige solid

**Melting point:** 263.3–264 °C

**$^{1}$H NMR** (600 MHz, DMSO-$d_6$): δ 11.27 (s, 1H, NHCO), 11.02 (s, 1H, NHCO), 8.58 (d, $J$ = 2.6 Hz, 1H, PzH), 8.37 (s, 1H, CONH), 8.34 (d, $J$ = 2.9 Hz, 1H, PzH), 7.99 (d, $J$ = 7.9 Hz, 2H, CONH, ArH), 7.25 (d, $J$ = 7.4 Hz, 1H, ArH), 7.20 (t, $J$ = 8.0 Hz, 1H, ArH), 7.04 (t, $J$ = 7.4 Hz, 1H, ArH), 2.36 (s, 3H, MeH).

**$^{13}$C NMR** (151 MHz, DMSO-$d_6$): δ 168.20, 151.54, 149.62, 144.43, 137.27, 135.98, 130.76, 129.78, 126.85, 126.55, 124.20, 121.75, 18.35.

**Elemental analysis:**

Theoretical Values: C: 57.56%, H: 4.83%, N: 25.82%

Experimental values: C: 57.09%, H: 4.92%, N: 25.01%.

**IR:** (ATR-Ge, cm$^{-1}$): 3411, 3203, 3045, 1697 (C=O, CONH), 1671 (C=O, CONH), 1581, 1563, 1540, 1478, 1460 (Aromatic).

**Compound 3:**

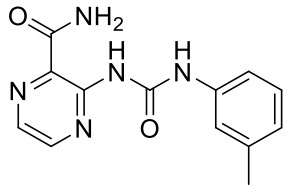

**Laboratory code:** 3-Me-VZN

**Chemical Name:** 3-(3-(*m*-tolyl)ureido)pyrazine-2-carboxamide

**Molecular weight:** 271.28 g/mol

**Yield:** 74 mg; 27.2%.

**Appearance:** beige solid

**Melting point:** 252.8–253.9 °C

**$^{1}$H NMR** (600 MHz, DMSO-$d_6$): δ 11.26 (s, 1H, NHCO), 11.10 (s, 1H, NHCO), 8.59 (d, $J$ = 2.5 Hz, 1H, PzH), 8.46 (s, 1H, CONH), 8.33 (d, $J$ = 2.5 Hz, 1H, PzH), 8.07 (s, 1H, CONH), 7.44–7.38 (m, 2H, ArH), 7.21 (t, $J$ = 7.7 Hz, 1H, ArH), 6.92–6.87 (m, 1H, ArH), 2.31 (s, 3H, MeH).

**$^{13}$C NMR** (151 MHz, DMSO-$d_6$): δ 167.51, 150.65, 148.83, 143.94, 137.99, 135.32, 128.93, 128.50, 123.89, 120.02, 116.71, 20.87.

**Elemental analysis:**

Theoretical Values: C: 57.56%, H: 4.83%, N: 25.82%

Experimental values: C: 57.11%, H: 4.93%, N: 26.16%.

**IR** (ATR-Ge, cm$^{-1}$): 3412, 3194, 1689 (C=O, CONH), 1656 (C=O, CONH), 1564, 1538, 1481, 1427 (Aromatic).

**Compound 4:**

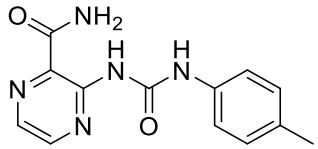

**Laboratory code:** 4-Me-VZN

**Chemical Name:** 3-(3-(*p*-tolyl)ureido)pyrazine-2-carboxamide

**Molecular weight:** 271.28 g/mol

**Yield:** 64 mg; 23.7%.

**Appearance:** white solid

**Melting point:** 226.0–228.5 °C

**$^{1}$H NMR** (600 MHz, DMSO-$d_6$): δ 11.31 (s, 1H, NHCO), 11.14 (s, 1H, NHCO), 8.59 (d, $J$ = 2.5 Hz, 1H, PzH), 8.57 (s, 1H, CONH), 8.33 (d, $J$ = 2.5 Hz, 1H, PzH), 8.17 (s, 1H, CONH), 7.52–7.46 (m, 2H, ArH), 7.18–7.11 (m, 2H, ArH), 2.27 (s, 3H, MeH).

**$^{13}$C NMR** (151 MHz, DMSO-$d_6$): δ 167.72, 150.83, 148.99, 144.14, 135.65, 135.47, 132.31, 129.27, 129.00, 119.64, 20.38.

**Elemental analysis:**

Theoretical Values: C: 57.56%, H: 4.83%, N: 25.82%

Experimental values: C: 56.81%, H: 4.836%, N: 25.92%.

**IR** (ATR-Ge, cm$^{-1}$): 3413, 3194, 1689 (C=O, CONH), 1659 (C=O, CONH), 1595, 1585, 1558, 1479 (Aromatic).

**Compound 5:**

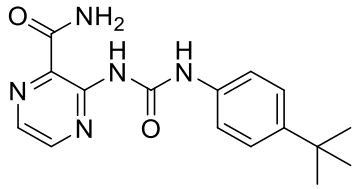

**Laboratory code:** 4-*t*-Bu-VZN

**Chemical Name:** 3-(3-(4-(*tert*-butyl)phenyl)ureido)pyrazine-2-carboxamide

**Molecular weight:** 313.36 g/mol

**Yield:** 80 mg; 25.5%.

**Appearance:** creamy color solid

**Melting point:** 232.4–233.8 °C

**$^{1}$H NMR** (600 MHz, DMSO-$d_6$): δ 11.32 (s, 1H, NHCO), 11.10 (s, 1H, NHCO), 8.59 (d, $J$ = 2.6 Hz, 1H, PzH), 8.57 (s, 1H, CONH), 8.33 (d, $J$ = 2.5 Hz, 1H, PzH), 8.17 (s, 1H, CONH), 7.54–7.47 (m, 2H, ArH), 7.38–7.32 (m, 2H, ArH), 1.27 (s, 9H, *tert*-BuH).

**$^{13}$C NMR** (151 MHz, DMSO-$d_6$): δ 167.73, 150.86, 149.00, 145.76, 144.16, 135.56, 135.48, 129.02, 125.49, 119.52, 33.99, 31.18.

**Elemental analysis:**

Theoretical Values: C: 61.33%, H: 6.11%, N: 22.35%

Experimental values: C: 60.92%, H: 5.995%, N: 22.11%.

**IR** (ATR-Ge, cm$^{-1}$): 3410, 3202, 2958, 1689 (C=O, CONH), 1658 (C=O, CONH), 1585, 1558, 1528, 1477 (Aromatic).

**Compound 6:**

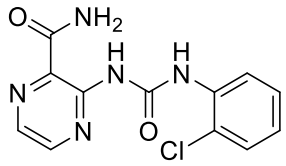

**Laboratory code:** 2-Cl-VZN

**Chemical Name:** 3-(3-(2-chlorophenyl)ureido)pyrazine-2-carboxamide

**Molecular weight:** 291.70 g/mol

**Yield:** 83 mg; 28.5%.

**Appearance:** white color solid

**Melting point:** 269.7–270 °C

**$^{1}$H NMR** (600 MHz, DMSO-$d_6$): δ 11.89 (s, 1H, NHCO), 11.51 (s, 1H, NHCO), 8.63 (m, 2H, PzH, CONH), 8.36 (m, 2H, PzH, CONH), 8.21 (m, 1H, ArH), 7.54 (d, $J$ = 7.9 Hz, 1H, ArH), 7.36 (t, $J$ = 7.7 Hz, 1H, ArH), 7.11 (t, $J$ = 7.9 Hz, 1H, ArH).

**$^{13}$C NMR:** Not available due to very bad solubility for $^{13}$C NMR measurement.

**Elemental analysis:**

Theoretical Values: C: 49.41%, H: 3.46%, N: 24.01%

Experimental values: C: 49.24%, H: 3.557%, N: 24.01%.

**IR:** (ATR-Ge, cm$^{-1}$): 3403, 3238, 3197, 1696 (C=O, CONH), 1672 (C=O, CONH), 1599, 1582, 1552, 1536, 1479, 1440 (Aromatic).

**Compound 7:**

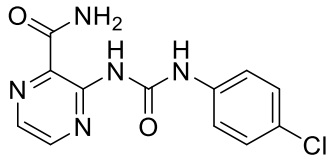

**Laboratory code:** 4-Cl-VZN

**Chemical Name:** 3-(3-(4-chlorophenyl)ureido)pyrazine-2-carboxamide

**Molecular weight:** 291.70 g/mol

**Yield:** 71 mg; 24.3%.

**Appearance:** creamy color solid

**Melting point:** 226–229 °C

**$^{1}$H NMR** (600 MHz, DMSO-$d_6$): δ 11.36 (s, 1H, NHCO), 11.27 (s, 1H, NHCO), 8.59 (d, $J$ = 2.6 Hz, 1H, PzH), 8.57 (s, 1H, CONH), 8.34 (d, $J$ = 2.5 Hz, 1H, PzH), 8.17 (s, 1H, CONH), 7.65 (d, $J$ = 8.5 Hz, 2H, ArH), 7.38 (d, $J$ = 8.6 Hz, 2H, ArH).

**$^{13}$C NMR** (151 MHz, DMSO-$d_6$): δ 167.69, 150.83, 148.83, 144.14, 137.24, 135.71, 129.10, 128.72, 126.92, 121.17.

**Elemental analysis:**

Theoretical Values: C: 49.41%, H: 3.46%, N: 24.01%

Experimental values: C: 48.51%, H: 3.504%, N: 23.68%.

**IR:** (ATR-Ge, cm$^{-1}$): 3407, 3189, 1689 (C=O, CONH), 1660 (C=O, CONH), 1584, 1559, 1538, 1475, 1435 (Aromatic).

**Compound 8:**

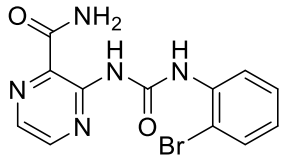

**Laboratory code:** 2-Br-VZN

**Chemical Name:** 3-(3-(2-bromophenyl)ureido)pyrazine-2-carboxamide

**Molecular weight:** 336.15 g/mol

**Yield:** 77 mg; 22.9%.

**Appearance:** white solid

**Melting point:** 270.1–271.5 °C

**$^{1}$H NMR** (600 MHz, DMSO-$d_6$): δ 11.72 (s, 1H, NHCO), 11.36 (s, 1H, NHCO), 8.63 (d, $J$ = 2.5 Hz, 1H, PzH), 8.39 (s, 1H, CONH), 8.37 (d, $J$ = 2.5 Hz, 1H, PzH), 8.32 (dd, $J$ = 8.3, 1.6 Hz, 1H, ArH), 8.01 (s, 1H, CONH), 7.67 (dd, $J$ = 8.0, 1.5 Hz, 1H, ArH), 7.39 (ddd, $J$ = 8.6, 7.3, 1.5 Hz, 1H, ArH), 7.05 (td, $J$ = 7.6, 1.6 Hz, 1H, ArH).

**$^{13}$C NMR** (151 MHz, DMSO-$d_6$): δ 167.23, 150.50, 148.26, 143.52, 136.61, 135.49, 132.15, 128.92, 127.85, 124.43, 121.43, 112.69.

**Elemental analysis:**

Theoretical Values: C: 42.88%, H: 3,00%, N: 20.83%

Experimental values: C: 42.82%, H: 3.068%, N: 20.6%.

**IR:** (ATR-Ge, cm$^{-1}$): 3402, 3196, 1730 (C=O, CONH), 1673 (C=O, CONH), 1578, 1552, 1481, 1435 (Aromatic).

**Compound 9:**

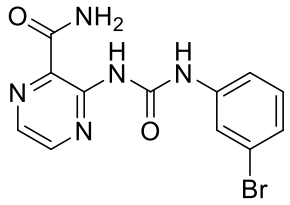

**Laboratory code:** 3-Br-VZN

**Chemical Name:** 3-(3-(3-bromophenyl)ureido)pyrazine-2-carboxamide

**Molecular weight:** 336.15 g/mol

**Yield:** 80 mg; 22.9%.

**Appearance:** creamy color solid

**Melting point:** 235.0–236.8 °C

**$^{1}$H NMR** (600 MHz, DMSO-$d_6$): δ 11.27 (s, 1H, NHCO), 11.20 (s, 1H, NHCO), 8.60 (d, $J$ = 2.5 Hz, 1H, PzH), 8.36 (s, 1H, CONH), 8.34 (d, $J$ = 2.5 Hz, 1H, PzH), 7.98 (s, 1H, CONH), 7.93 (t, $J$ = 2.0 Hz, 1H, ArH), 7.57 (ddd, $J$ = 8.0, 2.1, 1.1 Hz, 1H, ArH), 7.32–7.26 (m, 2H, ArH).

**$^{13}$C NMR** (151 MHz, DMSO-$d_6$): δ 168.19, 151.41, 149.41, 144.71, 140.55, 136.32, 131.20, 129.86, 126.51, 122.71, 122.21, 119.22.

**Elemental analysis:**

Theoretical Values: C: 42.88 %, H: 3.00 %, N: 20.83 %

Experimental values: C: 42.56 %, H: 3.038 %, N: 20.42 %.

**IR:** (ATR-Ge, cm$^{-1}$): 3412, 3198, 1696 (C=O, CONH), 1674 (C=O, CONH), 1593, 1580, 1551, 1537, 1481, 1473 (Aromatic).

**Compound 10:**

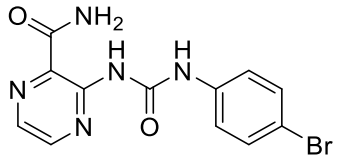

**Laboratory code:** 4-Br-VZN

**Chemical Name:** 3-(3-(4-bromophenyl)ureido)pyrazine-2-carboxamide

**Molecular weight:** 336.15 g/mol

**Yield:** 91 mg; 27.3%.

**Appearance:** creamy color solid

**Melting point:** 224.1–226.3 °C

**$^{1}$H NMR** (600 MHz, DMSO-$d_6$): δ 11.37 (s, 1H, NHCO), 11.28 (s, 1H, NHCO), 8.59 (d, $J$ = 2.5 Hz, 1H, PzH), 8.58 (s, 1H, CONH), 8.35 (d, $J$ = 2.5 Hz, 1H, PzH), 8.18 (s, 1H, CONH), 7.63–7.58 (m, 2H, ArH), 7.54–7.48 (m, 2H, ArH).

**$^{13}$C NMR** (151 MHz, DMSO-$d_6$): δ 167.69, 150.81, 148.81, 144.17, 137.69, 135.75, 131.63, 129.13, 121.54, 114.90.

**Elemental analysis:**

Theoretical Values: C: 42.88%, H: 3%, N: 20.83%

Experimental values: C: 42.43 %, H: 2.99%, N: 20.73 %

**IR** (ATR-Ge, cm$^{-1}$): 3401, 3197 (C=O, CONH), 1693, 1662 (C=O, CONH), 1597, 1582, 1557, 1537, 1475 (Aromatic).

**Compound 11:**

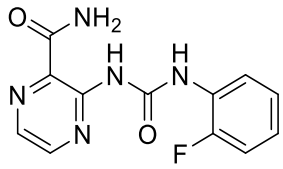

**Laboratory code:** 2-F-VZN

**Chemical Name:** 3-(3-(2-fluorophenyl)ureido)pyrazine-2-carboxamide

**Molecular Weight:** 275.24 g/mol

**Yield:** 77 mg; 28.1%.

**Purity (HPLC):** 99.82%

**Appearance:** white solid

**Melting point:** decomposed at 270 °C

**$^{1}$H NMR** (600 MHz, DMSO-$d_6$): δ 11.51 (s, 1H, NHCO), 11.47 (s, 1H, NHCO), 8.61 (s, 1H, CONH), 8.57 (d, $J$ = 2.5 Hz, 1H, PzH), 8.36 (d, $J$ = 2.5 Hz, 1H, PzH), 8.21 (s, 1H, CONH), 8.20–8.17 (m, 1H, ArH), 7.39–7.26 (m, 1H, ArH), 7.25–7.17 (m, 1H, ArH), 7.16–7.07 (m, 1H, ArH).

**$^{13}$C NMR** (151 MHz, DMSO-$d_6$): δ 167.65, 152.34 (d, $J$ = 242.8 Hz), 150.75, 148.76, 143.88, 135.84, 129.25, 126.35 (d, $J$ = 10.5 Hz), 124.72 (d, $J$ = 3.5 Hz), 124.00 (d, $J$ = 7.4 Hz), 121.42, 115.09 (d, $J$ = 18.9 Hz).

**Elemental analysis:** Not determined

**IR:** (ATR-Ge, cm$^{-1}$): 3414, 3132, 3045 (C=O, CONH), 1704, 1681 (C=O, CONH), 1564, 1537, 1479, 1457(Aromatic).

**Compound 12:**

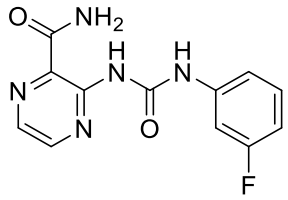

**Laboratory code:** 3-F-VZN

**Chemical Name:** 3-(3-(3-fluorophenyl)ureido)pyrazine-2-carboxamide

**Molecular weight:** 275.24 g/mol

**Yield:** 79 mg; 28.8%.

**Purity (HPLC):** 98.97%

**Appearance:** creamy color solid

**Melting point:** 227–229.7 °C

**$^{1}$H NMR** (600 MHz, DMSO-$d_6$): δ 11.30 (s, 1H, NHCO), 11.26 (s, 1H, NHCO), 8.59 (d, $J$ = 2.6 Hz, 1H, PzH), 8.40 (s, 1H, CONH), 8.34 (d, $J$ = 2.5 Hz, 1H, PzH), 8.02 (s, 1H, CONH), 7.58 (dt, $J$ = 11.7, 2.1 Hz, 1H, ArH), 7.39–7.32 (m, 2H. ArH), 6.91–6.84 (m, 1H, ArH).

**$^{13}$C NMR** (151 MHz, DMSO-$d_6$): δ 167.35, 162.09 (d, $J$ = 242.7 Hz), 150.55, 148.58, 143.84, 139.84 (d, $J$ = 11.6 Hz), 135.46, 130.04 (d, $J$ = 8.7 Hz), 128.99, 115.20, 109.40 (d, $J$ = 20.2 Hz), 106.27 (d, $J$ = 26.0 Hz).

**Elemental analysis:** Not determined

**IR:** (ATR-Ge, cm$^{-1}$): 3413, 3200, 1681 (C=O, CONH), 1661 (C=O, CONH), 1621, 1565, 1537, 1479, 1451 (Aromatic).

**Compound 13:**

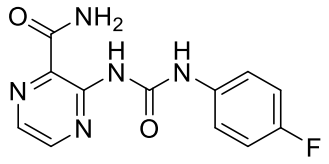

**Laboratory code:** 4-F-VZN

**Chemical Name:** 3-(3-(4-fluorophenyl)ureido)pyrazine-2-carboxamide

**Molecular weight:** 275.24 g/mol

**Yield:** 68 mg; 24.9%.

**Purity (HPLC):** 100%

**Appearance:** light yellow solid

**Melting point:** decomposed at 270 °C

**$^{1}$H NMR** (600 MHz, DMSO-$d_6$): δ 11.31 (s, 1H, NHCO), 11.18 (s, 1H, NHCO), 8.59 (d, $J$ = 2.5 Hz, 1H, PzH), 8.56 (s, 1H, CONH), 8.34 (d, $J$ = 2.5 Hz, 1H, PzH), 8.18 (s, 1H, CONH), 7.65–7.59 (m, 2H, ArH), 7.23–7.11 (m, 2H, ArH).

**$^{13}$C NMR** (151 MHz, DMSO-$d_6$): δ 167.71, 158.18 (d, $J$ = 239.8 Hz), 151.00, 148.91, 144.22, 135.67, 134.57, 129.09, 121.58 (d, $J$ = 8.2 Hz), 115.44 (d, $J$ = 22.9 Hz).

**Elemental analysis:** Not determined.

**IR** (ATR-Ge, cm$^{-1}$): 3414, 3132, 3045, 1681 (C=O, CONH), 1604 (C=O, CONH), 1564, 1537, 1479, 1457(Aromatic).

**Compound 14:**

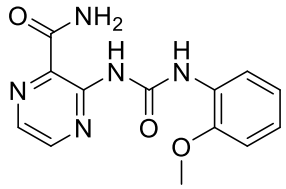

**Laboratory code:** 2-MeO-VZN

**Chemical Name:** 3-(3-(2-methoxyphenyl)ureido)pyrazine-2-carboxamide

**Molecular weight:** 287.28 g/mol

**Yield:** 77 mg; 26.8%.

**Appearance**: creamy color solid

**Melting point:** 237.8–240.2 °C

**$^{1}$H NMR** (600 MHz, DMSO-$d_6$): δ 11.60 (s, 1H, NHCO), 11.30 (s, 1H, NHCO), 8.62 (d, $J$ = 2.5 Hz, 1H, PzH), 8.46 (s, 1H, CONH), 8.34 (d, $J$ = 2.5 Hz, 1H, PzH), 8.21 (dd, $J$ = 8.0, 1.6 Hz, 1H, ArH), 8.08 (s, 1H, CONH), 7.09–7.00 (m, 2H, ArH), 6.94 (td, $J$ = 7.6, 1.6 Hz, 1H, ArH), 3.95 (s, 3H, OMeH)

**$^{13}$C NMR** (151 MHz, DMSO-$d_6$): δ 167.50, 150.53, 146.55, 143.84, 135.34, 130.83, 127.81, 125.75, 122.95, 120.52, 118.77, 110.90, 56.06.

**Elemental analysis:**

Theoretical Values: C: 54.35%, H: 4.56%, N: 24.38%

Experimental values: Not determined.

**IR:** (ATR-Ge, cm$^{-1}$): 3415, 3197, 1691 (C=O, CONH), 1673 (C=O, CONH), 1607, 1580, 1557, 1481, 1434 (Aromatic).

**Compound 15:**

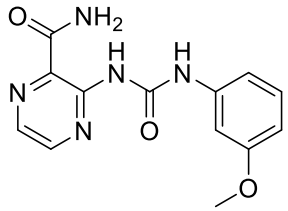

**Laboratory code:** 3-MeO-VZN

**Chemical Name:** 3-(3-(3-methoxyphenyl)ureido)pyrazine-2-carboxamide

**Molecular weight:** 287.28 g/mol

**Yield:** 78 mg; 27.4%.

**Purity (HPLC): Not available.**

**Appearance**: Beige solid

**Melting point:** 216.9–218.6 °C

**$^{1}$H NMR** (600 MHz, DMSO-$d_6$): δ 11.34 (s, 1H, NHCO), 11.21 (s, 1H, NHCO), 8.61 (d, $J$ = 2.5 Hz, 1H, PzH), 8.58 (s, 1H, CONH), 8.34 (d, $J$ = 2.5 Hz, 1H, PzH), 8.17 (s, 1H, CONH), 7.30 (t, $J$ = 2.3 Hz, 1H, ArH), 7.24 (t, $J$ = 8.1 Hz, 1H, ArH), 7.14 (dd, $J$ = 7.9, 2.0 Hz, 1H, ArH), 6.66 (dd, $J$ = 8.2, 2.5 Hz, 1H, ArH), 3.76 (s, 3H, OMeH).

**$^{13}$C NMR** (151 MHz, DMSO-$d_6$): (151 MHz, DMSO-$d_6$) δ 167.72, 159.72, 150.81, 148.93, 144.17, 139.41, 135.60, 129.67, 129.06, 111.91, 108.68, 105.52, 55.09.

**Elemental analysis:**

Theoretical Values: C: 54.35%, H: 4.56%, N: 24.38%

Experimental values: Not determined.

**IR:** (ATR-Ge, cm$^{-1}$): 3410, 3247, 3203, 2833, 1687 (C=O, CONH), 1658 (C=O, CONH), 1595, 1568, 1477, 1451 (Aromatic).

**Compound 16:**

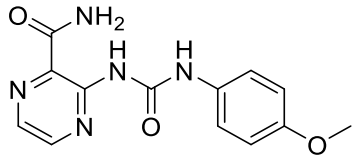

**Laboratory code:** 4-MeO-VZN

**Chemical Name:** 3-(3-(4-methoxyphenyl)ureido)pyrazine-2-carboxamide

**Molecular weight:** 287.28 g/mol

**Yield:** 79 mg; 27.5%.

**Appearance:** light yellow solid

**Melting point:** 223–226.3 °C

**$^{1}$H NMR** (600 MHz, DMSO- $d_6$): δ 11.28 (s, 1H, NHCO), 11.02 (s, 1H, NHCO), 8.58 (d, $J$ = 2.6 Hz, 1H, PzH), 8.57 (s, 1H, CONH), 8.32 (d, $J$ = 2.5 Hz, 1H, PzH), 8.16 (s, 1H, CONH), 7.53–7.47 (m, 2H, ArH), 6.94–6.89 (m, 2H, ArH), 3.74 (s, 3H, OMeH).

**$^{13}$C NMR** (151 MHz, DMSO- $d_6$): δ 167.74, 155.46, 150.95, 149.03, 144.16, 135.40, 131.14, 128.95, 121.44, 114.04, 55.21.

**Elemental analysis:**

Theoretical Values: C: 54.35%, H: 4.56%, N: 24.38%

Experimental values: C: 54.24%, H: 4.531%, N: 23.77%.

**IR** (ATR-Ge, cm$^{-1}$): 3432, 3203, 2963, 2841, 1698 (C=O, CONH), 1668 (C=O, CONH), 1605, 1584, 1567, 1511, 1478 (Aromatic).

**Compound 17:**

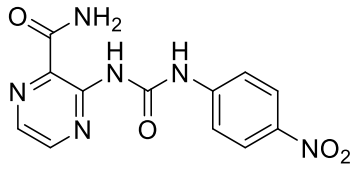

**Laboratory code:** 4-nitro-VZN

**Chemical Name:** 3-(3-(4-nitrophenyl)ureido)pyrazine-2-carboxamide

**Molecular weight:** 302.25 g/mol

**Yield:** 89 mg; 29.4%.

**Appearance:** yellow solid

**Melting point:** 231–233.9 °C

**$^{1}$H NMR** (600 MHz, DMSO-$d_6$): δ 11.67 (s, 1H, NHCO), 11.51 (s, 1H, NHCO), 8.63 (d, $J$ = 2.5 Hz, 1H, PzH), 8.60 (s, 1H, CONH), 8.39 (d, $J$ = 2.5 Hz, 1H, PzH), 8.25–8.22 (m, 2H, ArH), 8.21 (s, 1H, CONH), 7.92–7.86 (m, 2H, ArH).

**$^{13}$C NMR** (151 MHz, DMSO-$d_6$): δ 167.65, 150.67, 148.59, 144.78, 144.25, 142.20, 136.20, 129.42, 125.00, 119.11.

**Elemental analysis:**

Theoretical Values: C: 47.69%, H: 3.33%, N: 27.81%

Experimental values: Not determined.

**IR:** 3450, 3124, 1702 (C=O, CONH), 1671 (C=O, CONH), 1599, 1563, 1508, 1468 (Aromatic).

## 6.6. Selected NMR Spectra of Some Prepared Compounds

**Compound-**1 (H-VZN)

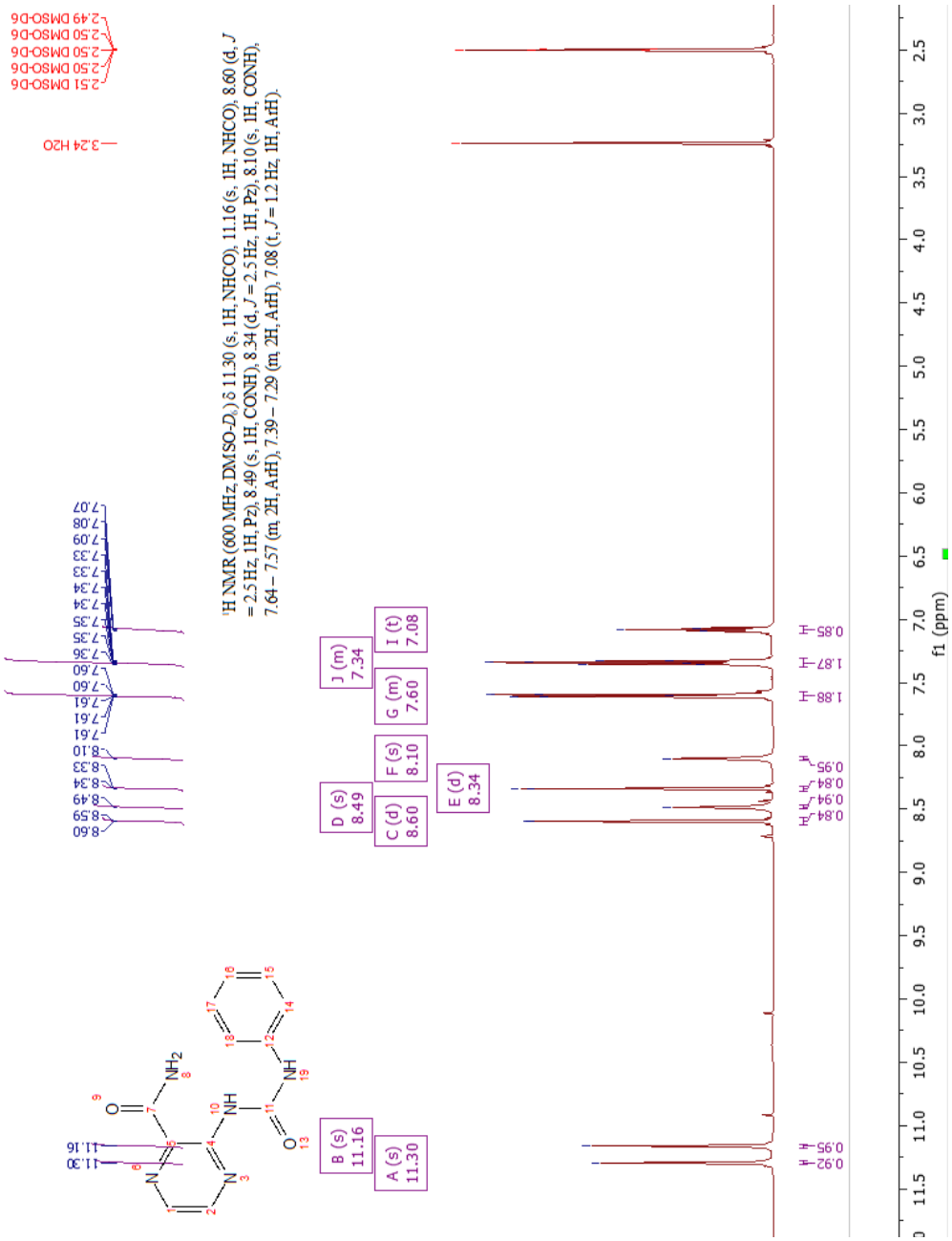

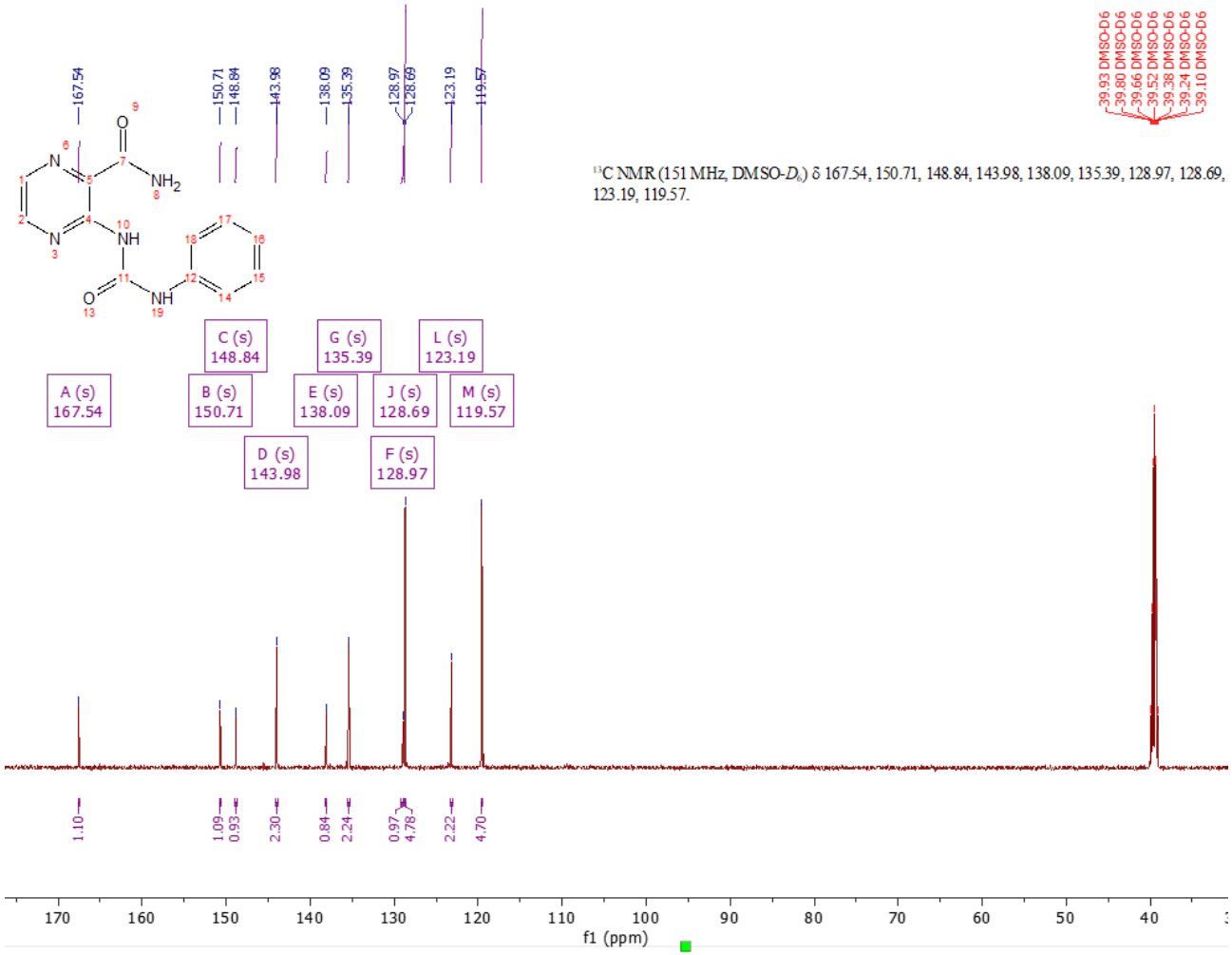


$^{13}$C NMR (151 MHz, DMSO-$D_6$) δ 167.54, 150.71, 148.84, 143.98, 138.09, 135.39, 128.97, 128.69, 123.19, 119.57.

**Compound-**3 (3-Me-VZN)

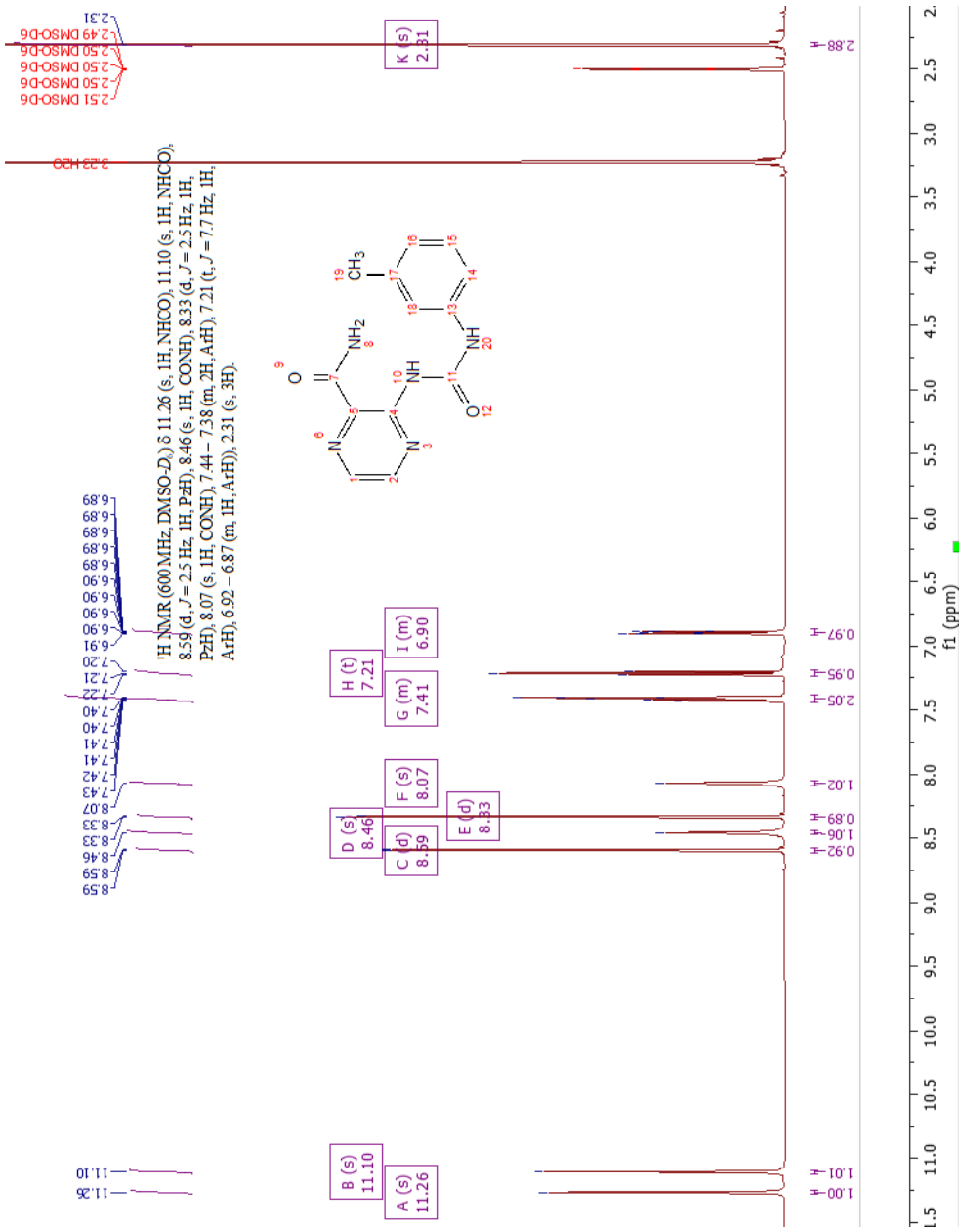

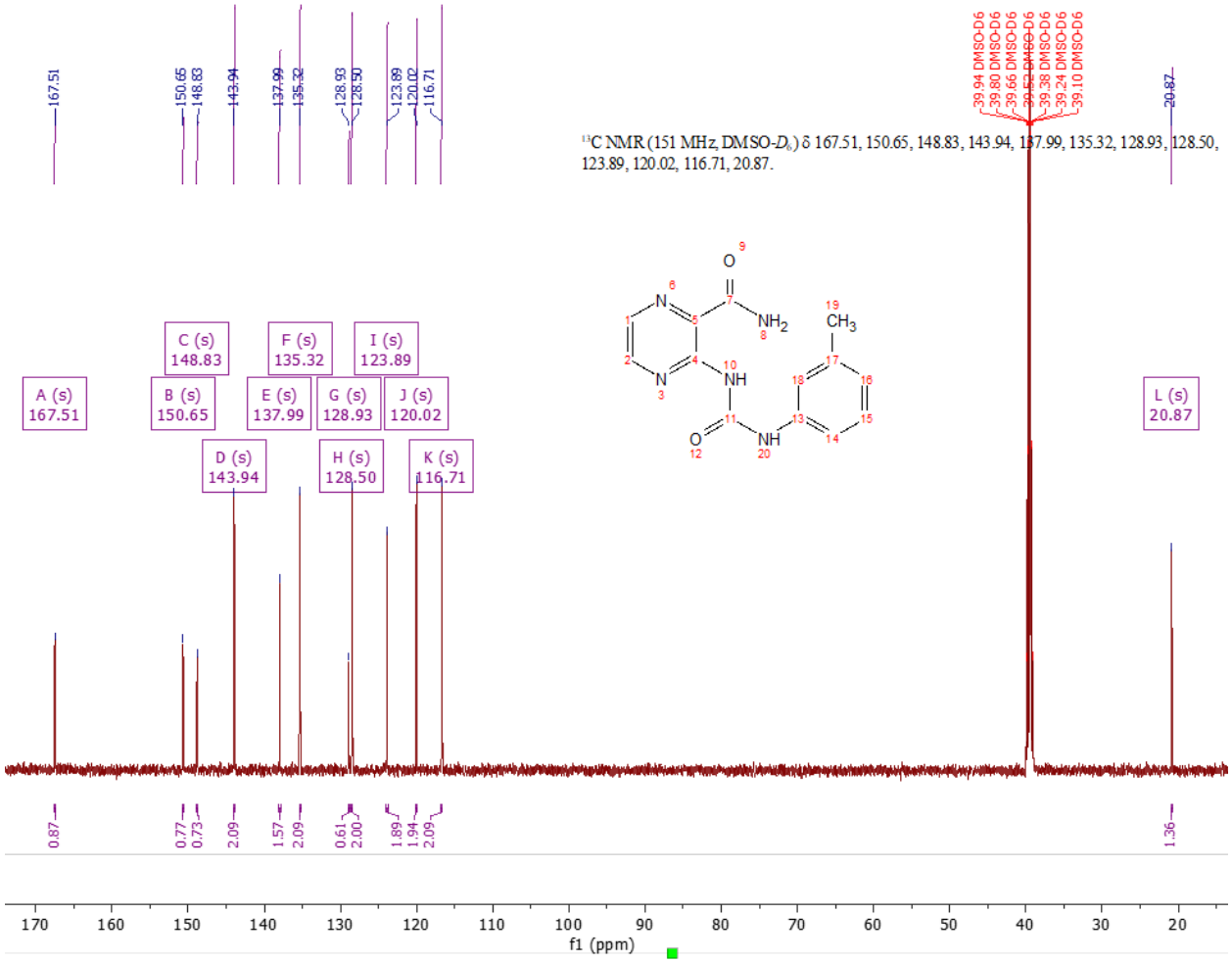
167.51
150.65
148.83
143.94
137.99
135.32
128.93
128.50
123.89
120.02
116.71
39.94 DMSO-D6
39.80 DMSO-D6
39.66 DMSO-D6
39.52 DMSO-D6
39.38 DMSO-D6
39.24 DMSO-D6
39.10 DMSO-D6
20.87
13C NMR (151 MHz, DMSO-D6) δ 167.51, 150.65, 148.83, 143.94, 137.99, 135.32, 128.93, 128.50, 123.89, 120.02, 116.71, 20.87.
A (s) 167.51
B (s) 150.65
C (s) 148.83
D (s) 143.94
E (s) 137.99
F (s) 135.32
G (s) 128.93
H (s) 128.50
I (s) 123.89
J (s) 120.02
K (s) 116.71
L (s) 20.87
0.87
0.77
0.73
2.09
1.57
2.09
0.61
2.00
1.89
1.94
2.09
1.36
170 160 150 140 130 120 110 100 90 80 70 60 50 40 30 20
f1 (ppm)

**Compound-**5 (4-*t*-Bu-VZN)

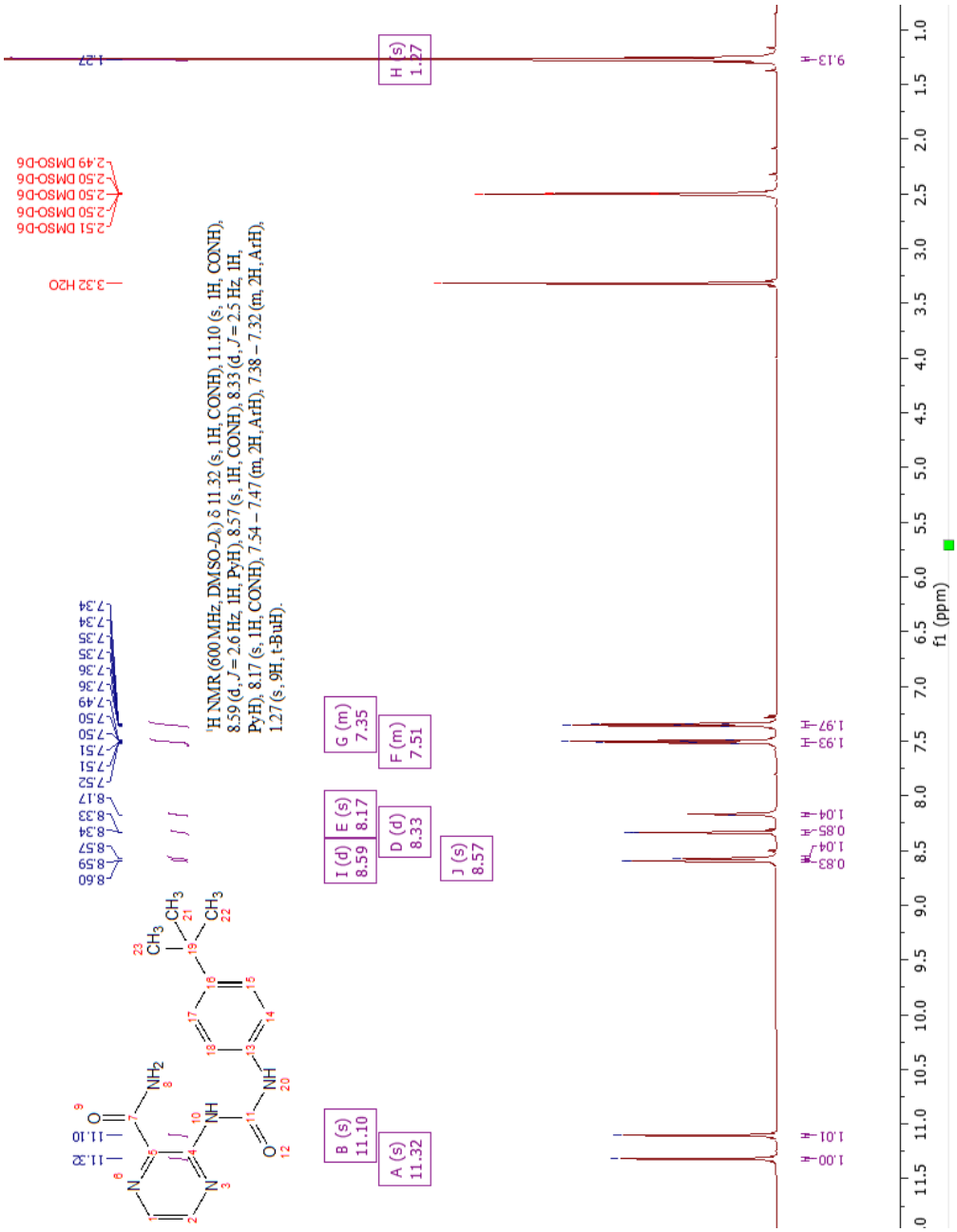

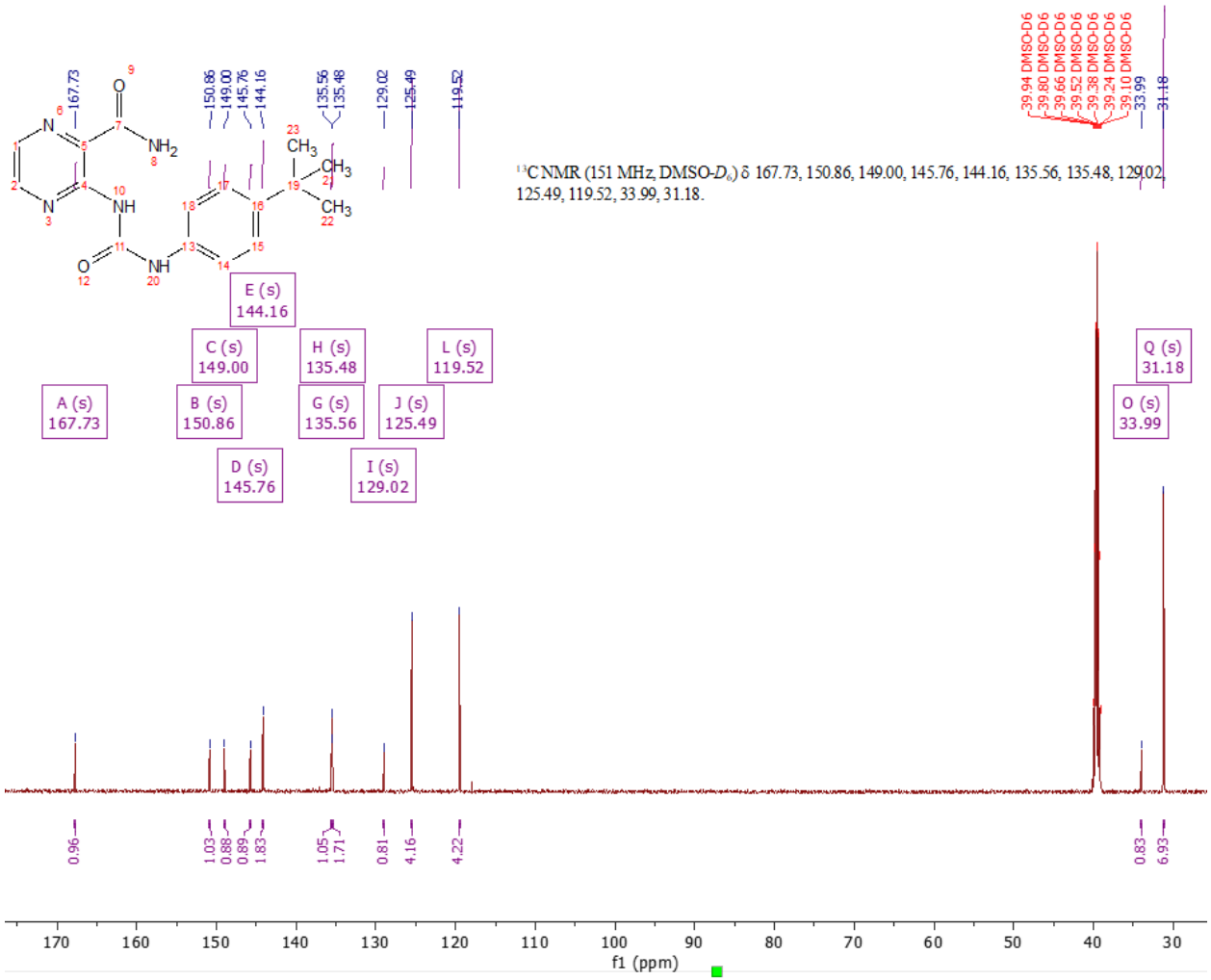
167.73
150.86
149.00
145.76
144.16
135.56
135.48
129.02
125.49
119.52
39.94 DMSO-D6
39.80 DMSO-D6
39.66 DMSO-D6
39.52 DMSO-D6
39.38 DMSO-D6
39.24 DMSO-D6
39.10 DMSO-D6
33.99
31.18
13C NMR (151 MHz, DMSO-D6) δ 167.73, 150.86, 149.00, 145.76, 144.16, 135.56, 135.48, 129.02, 125.49, 119.52, 33.99, 31.18.
A (s) 167.73
B (s) 150.86
C (s) 149.00
D (s) 145.76
E (s) 144.16
G (s) 135.56
H (s) 135.48
I (s) 129.02
J (s) 125.49
L (s) 119.52
O (s) 33.99
Q (s) 31.18
0.96
1.03
0.88
0.89
1.83
1.05
1.71
0.81
4.16
4.22
0.83
6.93
170
160
150
140
130
120
110
100
90
80
70
60
50
40
30
f1 (ppm)

# 7. Results and discussion

## 7.1. Chemistry

3-chloropyrazine-2-carboxamide as a starting compound was synthesized from 3-chloropyrazine-2-carbonitrile by partial hydrolysis of the nitrile group under defined pH and temperature [39].

The choice of the procedure to get the starting compound other than direct amidation of the pyrazine ring was because of the yield percentage [37].

Synthesis of 3-aminopyrazin-2-carboxamide has been done through chemical substitution reaction between the starting compound and $NH_3$ in MeOH using a microwave reactor (scheme 4)**.**

Then, to have different substituted phenyl 3-phenylureidopyrazine-2-carboxamides, many solvents and conditions have been tried like; hexane, THF, DMSO and ACN. Also, the reaction in neat (without using solvent) was tried, but the yield percentage wasn't good, and carbonation was another problem.

Lastly, using anhydrous acetonitrile (ACN) as a solvent was successful and the yield percentage was almost 20–30%. The obtained final compounds are solid and generally less soluble in organic solvents. Hence they were purified by washing with water, different organic solvents, followed by precipitation techniques were used for compounds containing halogen substitutions which are very bad soluble. While rest of the compounds with alkyl substutions with higher solubilty in organic solvents were purified in flash chromatography (Hex/EtOAc gradient mobile phase) followed precipitation technique using acetone/hexane. All the final compounds were characterized using NMR spectroscopy and IR spectroscopy. The purity of the all final compounds were tested by measuring the elemental composition using elemental analysis, while compounds with fluorine atom were measured on HPLC.

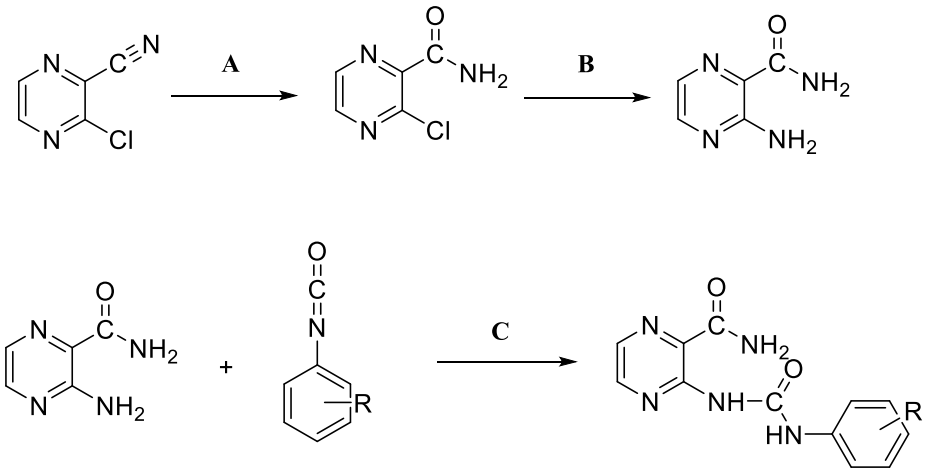

**Scheme 4:** synthesis of final compounds. Reagents and conditions:
**(A)** $H_2O_2$ (30%), $H_2O$, pH 9, 3 hr at 50-55°C;
**(B)** $NH_3$ in MeOH, MW: Pressure: 150psi, 120 °C, and Power: 150W;
**(C)** Anhyd. ACN, MW: Pressure: 150psi, 120 °C, and Power: 150W.

## 7.2. Biological evaluation

### In Vitro Antimycobacterial Evaluation

*Mtb* H37Ra (avirulent strain)*, M. avium, M. kansasi, M. aurum, M. smegmatis, and M. aurum* were used for antimicrobial screening in vitro, using a modified Microplate Alamar Blue Assay (MABA).

After diluting all compounds to final concentrations by serial dilution technique as; 500-250-125-62.5-31.25-15.62-7.81-3.91-1.95 µg/mL, they were compared to standards; rifampicin (RIF), isoniazid (INH), and ciprofloxacin (CIP). Antimycobacterial activity was measured as MIC in µg/ml.

10 out of 17 compounds, substituted and non-substituted of 3-phenylureidopyrazine-2-carboxamide, were tested, but the majority of them were non-active or showing minimal activity, except for some which they showed moderate to low activities like; 4-*tert*-Bu (MIC 62.5 µg/mL for *M. kansasi*), 4-$NO_2$ (MIC 62.5 µg/mL for *M. avium*), 4-Br (MIC 250 µg/mL for *M. avium*), 4-Cl (MIC 250 µg/mL for *M. avium*), 2-F (MIC 250 µg/mL for *M. avium*), and non-substituted (MIC 500 µg/mL *M. avium*). See Table-1 for results.

**Table 1:** Antimycobacterial activities of prepared compounds.

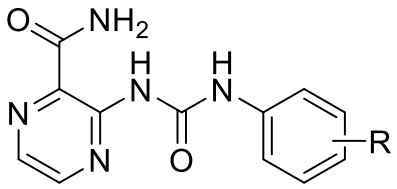

| Code | R | *M. smeg.* MIC (µg/mL) | *M. aurum* MIC (µg/mL) | *M. avium* MIC (µg/mL) | *M. kansasii* MIC (µg/mL) | *M. tb* H37Ra MIC (µg/mL) | CLog P |
|---|---|---|---|---|---|---|---|
| **5** | 4-t-Bu | ≥ 500 | ≥ 500 | ≥ 500 | 62.5 | ≥ 500 | 3.62 |
| **4** | 4-Me | ≥ 125 | ≥ 125 | ≥ 125 | ≥ 125 | ≥ 125 | 2.29 |
| **2** | 2-Me | ≥ 500 | ≥ 500 | ≥ 500 | ≥ 500 | ≥ 500 | 1.73 |
| **10** | 4-Br | ≥ 500 | ≥ 500 | 250 | ≥ 500 | ≥ 500 | 2.67 |
| **16** | 4-MeO | ≥ 500 | ≥ 500 | ≥ 500 | ≥ 500 | ≥ 500 | 1.72 |
| **1** | H | ≥ 500 | ≥ 500 | 500 | ≥ 500 | ≥ 500 | 1.79 |
| **11** | 2-F | ≥ 500 | ≥ 500 | 250 | ≥ 500 | ≥ 500 | 1.50 |
| **13** | 4-F | ≥ 500 | ≥ 500 | ≥ 500 | ≥ 500 | ≥ 500 | 1.95 |
| **7** | 4-Cl | ≥ 500 | ≥ 500 | 250 | ≥ 500 | ≥ 500 | 2.52 |
| **17** | 4-$NO_2$ | ≥ 500 | ≥ 500 | 62.5 | 500 | ≥ 500 | 2.29 |
| **INH** | - | 15.625 | 3.91 | 1000 | 6.25 | 0.25 | - |
| **RIF** | - | 12.5 | 0.39 | 0.25 | 0.025 | 0.00313 | - |
| **CIP** | - | 0.125 | 0.015625 | 0.78 | 0.25 | 0.25 | - |

**Standards:** CIP: ciprofloxacin, RIF: rifampicin, INH: isoniazid. Clog P – calc. from ChemDraw

Our compounds are analogues of recently published 3-benzamidopyrazine-2-carboxamides, where the only difference with our compounds is the one atom extended urea linker instead of the amidic linker in the previous series (Figure 11).

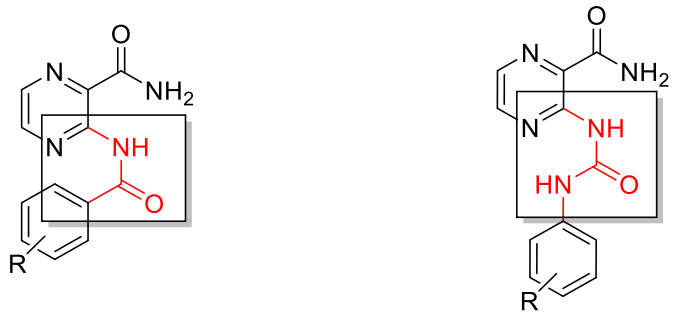


**Figure 11: Left:** published 3-benzamidopyrazine-2-carboxamide derivatives; **Right:** 3-(3-phenylureido)pyrazine-2-carboxamide derivatives (our compounds).

Regarding the published results, we can see various activities with different positions and substitutions; 2nd, 3rd and 4th, but most active ones were with 4th positions.

In our series, we don't have results for all compounds from all positions, but as we noticed in the currently available biological results, extending the linker had a negative impact on antimycobacterial activity for most substituents and positional isomers. For 2'-substituted derivatives and unsubstituted derivatives, we can't see much difference, mainly because these substitutions were inactive even in the original 3-benzamide series. For example, in the case of 2'-F substitution, the compounds showed low activity in both series (MIC 250 µg/mL) and for unsubstituted compounds, the activity was very low, in a way for ours showed (MIC 500 µg/mL) against *M. avium,* and for published one showed (MIC 250 µg/mL) against *M. H37Ra* strain.

For the third position, we don't have results for our compounds, but regarding the 4th position, where the most active ones from published article were from this position, decreased activity can been seen in our compounds (as it shown in Table-2) [1].

**Table 2:** Comparison between activity between our compounds (left) and published compounds (right) against *Mtb* H37Ra.

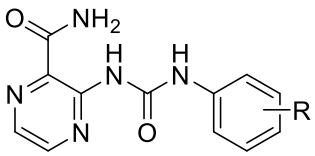

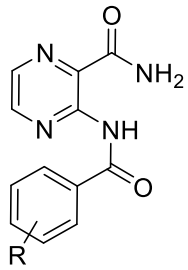

| Code | R | *Mtb* H37Ra MIC (µg/mL) | R | *Mtb* H37Ra MIC (µg/mL) |
|---|---|---|---|---|
| **5** | 4-*tert*-Bu | ≥ 500 | 4-*tert*-Bu | 15.625 |
| **4** | 4-Me | ≥ 125 | 4-Me | 7.81 |
| **10** | 4-Br | ≥ 500 | 4-Br | 1.95 |
| **16** | 4-$OCH_3$ | ≥ 500 | 4-$OCH_3$ | ≥ 125 |
| **13** | 4-F | ≥ 500 | 4-F | 31.25 |
| **7** | 4-Cl | ≥ 500 | 4-Cl | 3.91 |
| **17** | 4-$NO_2$ | ≥ 500 | 4-$NO_2$ | 125 |
| **INH** | - | 0.25 | - | |
| **RIF** | - | 0.00313 | - | |
| **CIP** | - | 0.25 | - | |

**Standards:** CIP: ciprofloxacin, RIF: rifampicin, INH: isoniazid.

## 7.3. In Silico Simulations

### Docking to Homology Model of Mycobacterial ProRS

To determine the possibility of interactions between our 3-(3-phenylureido)pyrazine-2-carboxamide derivates (including all tested and virtually prepared) and mycobacterial ProRS (mtProRS), molecular docking was performed into a homology model of mtProRS.

Because the crystallographic structure of the protein (mtProRS) wasn't available, the homology model, which was constructed by AlphaFold (an artificial intelligence), was used [40].

The receptor system was prepared in a recently published article, where they used bacterial ProRS of *Enterococcus faecalis* as a template to manipulate proline and adenosine as a substrate and a substrate-like structure, respectively, into the homology structure [1]. The existence of a crystallographic water molecule (mediating the interactions between adenosine and the protein) was derived from various homologous structures of ProRSs. The importance of this water molecule was also confirmed by Solvent Analysis application using 3D-RISM model [41]. This made us preserve this one water molecule.

According to the results of a recently published article, the most active compounds exerted a consistent binding mode, which included the main interactions: Ala154 HBA and Ala154 HBD and some other additional interactions (Figure 12) [1]. Therefore, the resulting docking poses of our compounds were filtered to have the same interactions.

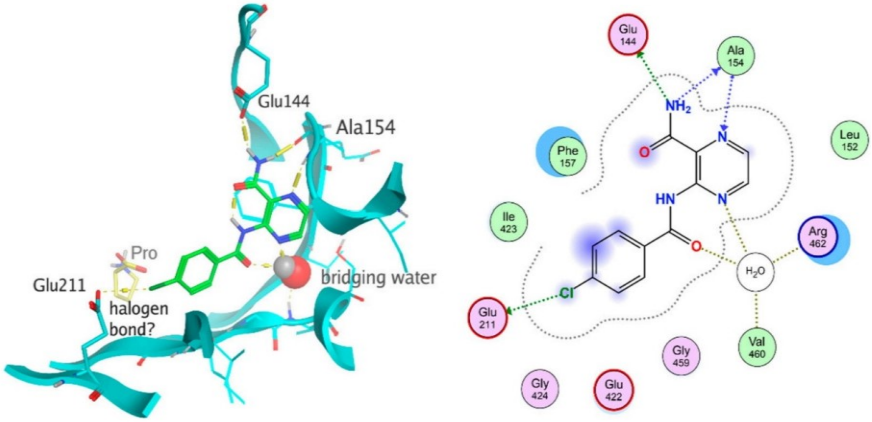


**Figure 12:** Ligand-protein interaction of 3-(4-chlorobenzamido)pyrazine-2-carboxamide with mtProRS in 3D depiction and in 2D diagram. Taken from the reference article [1].

Based on our docking results, 25 out of 57 3-(3-phenylureido)pyrazine-2-carboxamides had the required interactions as well as some other interactions – see Table-3.

**Table 3:** Docking to a homology model of mtProRS – 25 best scored compounds.

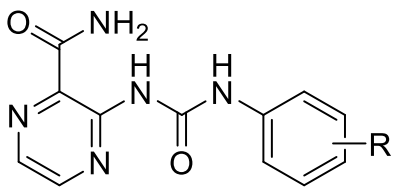


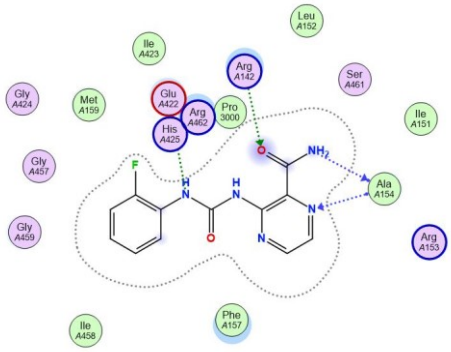


| Virt. code/ No. | R | Ala154 HBA | Ala154 HBD | IMHB | Additional interactions | Score | Rank |
|---|---|---|---|---|---|---|---|
| Cpd 11 | 2-F | + | + | + | 1. Arg142 HBA (carbonyl oxygen of pyrazinamide). | -7.397 | 2 |
| V1 | 2-OH | + | + | + | 1. Arg142 HBA (carbonyl oxygen)<br>2. Pro 3000 HBA (with 2-OH) | -7.350 | 1 |
| V2 | 2-*i*Pr | + | + | + | Arg142 HBA (carbonyl oxygen of pyrazinamide). | -7.327 | 1 |
| V3 | 2-$NH_2$ | + | + | - | 1. Arene (pyrazin)-arene (Phe157) interaction.<br>2. Arg142 HBA (carbonly oxygen of amide). | -6.960 | 2 |
| Cpd 1 | H | + | + | + | 1. Arene(pyrazin)-arene (Phe A157) interaction.<br>2. Arg142 HBA (carbonly oxygen of amide). | -7.060 | 2 |
| Cpd 12 | 3-F | + | + | - | 1. Arg142 HBA (carbonly oxygen of amide). | -6.893 | 3 |
| V4 | 5-F-2-Me | + | + | + | 1. Arene (pyrazin)-arene (Phe A157) interaction. | -7.174 | 1 |
| V5 | 2-F-6-Me | + | + | + | 1. Arene (pyrazin)-arene (Phe A157) interaction. | -7.162 | 1 |

| | | | | | | | |
|---|---|---|---|---|---|---|---|
| Cpd 2 | 2-Me | + | + | + | 1. Arene (pyrazin)-arene (Phe A157) interaction. | -7.097 | 1 |
| V6 | 2-Me-4-F | + | + | + | 1.Arene (pyrazin)-arene (Phe A157) interaction.<br>2. Glu144 HBD ($NH_2$ of amide) | -7.0870 | 1 |
| V7 | 3,5-diF | + | + | - | 1. Arene (pyrazin)-arene (Phe A157) interaction.<br>2. Glu144 HBD ($NH_2$ of amide) | -7.041 | 1 |
| V8 | quinoline-based derivative, see Fig. 13 for structure. | + | + | + | 1.Arg142 HBA (carbonyl oxygen).<br>2. Arene (pyrazin)-arene (Phe A157) interaction.<br>3. Glu144 HBD ($NH_2$ of amide).<br>4. Pro 3000 HBD (pyridine nitrogen).<br>5. ionic interaction between pyridin nitrogen and Glu422.<br>6. ionic interaction between urea NH group and Glu422. | -7.039 | 1 |
| V9 | 3,4-diOH | + | + | - | 1. Glu422 HBD (3-OH)<br>2. Glu144 HBD ($NH_2$ group of amide). | -7.011 | 1 |
| V10 | 2-$NH_2$-4-OH | + | + | - | 1. Glu422 HBD (2-amino).<br>2. Ile423 HBD (HBA (2-amino).<br>3. Pro 3000 HBA (with 4-OH).<br>4. Arg 142 HBA (carbonly oxygen of amide). | -6.972 | 1 |
| V11 | 3-OH | + | + | + | 1. Arg142 HBA (carbonly oxygen of amide). | -6.926 | 1 |
| V12 | 3-$NH_2$ | + | + | - | 1. Arg142 HBA (carbonly oxygen of amide). | -6.922 | 1 |
| Cpd 13 | 4-F | + | + | - | 1. Arg142 HBA (carbonly oxygen of amide).<br>2. Glu422 HBD with urea NH group. | -6.873 | 1 |
| V13 | 2-OH-3,5-diCl | + | + | + | 1. Pro 3000 HBD (with 2-OH).<br>2. Arene (pyrazin)-arene (Phe A157) interaction.<br>3. Arg142 HBD (carbonly oxygen of amide). | -6.868 | 1 |

| | | | | | | | |
|---|---|---|---|---|---|---|---|
| Cpd 6 | 2-Cl | + | + | - | 1. Glu422 HBA (with urea NH group). 2. Arg142 HBD (with carbonly oxygen of amide). | -6.830 | 1 |
| V14 | 2-Et | + | + | | 1. Glu422 HBA (with urea NH group). 2. Arene (pyrazin)-arene (Phe A157) interaction, Arg142 HBD (with carbonly oxygen of amide). | -6.806 | 1 |
| Cpd 5 | 4-*t*-Bu | + | + | + | 1. Arene (pyrazin)-arene (Phe A157) interaction.<br>2. Arg142 HBD (with carbonly oxygen of amide). | -6.756 | 1 |
| V15 | 2-Me-3-Cl | + | + | - | 1. Arene (pyrazin)-arene (Phe A157) interaction.<br>2. Glu144 HBA (with $NH_2$ of amide). | -6.726 | 1 |
| V16 | 2-Me-4-Cl | + | + | + | 1. Arene (pyrazin)-arene (Phe A157) interaction.<br>2. Arg142 HBD (with carbonly oxygen of amide). | -6.618 | 1 |
| V17 | 2-Cl-6-Me | + | + | - | 1. Arene (pyrazin)-arene (Phe157) interaction.<br>2. Arg142 HBD (with carbonly oxygen of amide). | -6.491 | 1 |
| Cpd 10 | 4-Br | + | + | - | 1. Arg142 HBD (with carbonly oxygen of amide). | -6.302 | 1 |

**Cpd:** compound (compounds synthesized in lab),
**V:** virtual (for virtually tested, not synthesized compounds),
**Rank:** rank by docking score of the described pose within all poses for the compound

13 compounds out of 25 have intramolecular H-bonding (IMHB) including the best three scored ones too, which gives the molecule more stability (less energetic state). And other additional interactions are mostly with Arg142, proline substrate, Glu144, Phe157 and Ile423. But most interesting is the ionic interaction of compound V8, 3-(3-(quinolin-7-yl)ureido)pyrazine-2-carboxamide, between the protonated quinoline nitrogen and Glu422 (Figure 13).

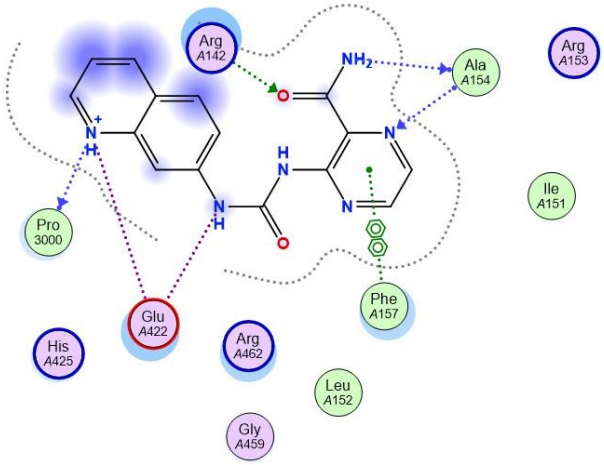


**Figure 13:** 2D diagram of compound V8, showing ionic interaction and some others.

13 compounds out of 25 are substituted on position 2' (including the first four compounds, 2-F, 2-OH, 2-isopropyl and 2-amino).

From these 25 compounds, we could synthesize and biologically test 6 compounds which were 2-F, H, 2-Me, 4-Br, 4-F, 4-*tert*-Bu, but the results didn't correlate with the computational docked compounds for some reasons which might be due to:

1. Docking in theory can predict the affinity to the receptor. So it can correlate with enzyme inhibition data. But it isn't expected to be correlated to the antimycobacterial activity on whole cells, because docking does not reflect the penetration into mycobacteria, efflux mechanism, metabolization of the compound by mycobacteria, etc.
2. Using the homology model of the protein, instead of crystallographic one due to unavailability.
3. Imperfection of computational modelling till now.
4. Errors in docking theories.
5. Other undefined parameters that may affect the results.

# 8. Conclusion

To sum up, 17 compounds of 3-(phenylureido)pyrazine-2-carboxamide derivatives, were synthesized, and 10 compounds were tested biologically against different strains of mycobacteria. As a complementary study, all the compounds were studied for *in silico* docking studies to observe binding towards mycobacterial ProRS.

As it shown, extension of the linker, turned to be unfavorable, and had impacts on decreasing activity. Also promising docking results aren't in agreement with the antimycobacterial activity.

Substituting the linker with a different and shorter group and using crystallographic model of the receptor instead of homology model for *in silico* simulations could help to synthesize promising compounds in the future.

# 9. References


1. Pallabothula, V.S.K., et al., *Adenosine-Mimicking Derivatives of 3-Aminopyrazine-2-Carboxamide: Towards Inhibitors of Prolyl-tRNA Synthetase with Antimycobacterial Activity.* Biomolecules, 2022. **12**(11): p. 1561.
2. Shrivastava, S.R., P.S. Shrivastava, and J. Ramasamy, *World health organization releases global priority list of antibiotic-resistant bacteria to guide research, discovery, and development of new antibiotics.* Journal of Medical Society, 2018. **32**(1): p. 76.
3. Williams, J., et al., *Phage Therapy Administration Route, Regimen, and Need for Supplementary Antibiotics in Patients with Chronic Suppurative Lung Disease.* PHAGE, 2023. **4**(1): p. 4-10.
4. Wei, S., et al., *Tuberculosis research and innovation: Interpretation of the WHO Global Tuberculosis Report 2021.* 2022 [cited 2023 04/06].
5. Cook, G.M., et al., *Physiology of mycobacteria.* Advances in microbial physiology, 2009. **55**: p. 81-319.
6. Herchline, T.E. and M.S. Bronze, *Tuberculosis (TB).* Medscape, 2019 [cited 2023 04/05]. https://emedicine.medscape.com/article/230802-overview
7. Jameson, J.L., et al., *Harrison's Principles of Internal Medicine, Twentieth Edition (Vol.1 & Vol.2)*. 2018: McGraw-Hill Education.
8. W.H.O., *Global investments in tuberculosis research and development: past, present and future. A policy paper prepared for the first WHO global ministerial conference on ending tuberculosis in the sustainable development era: a multisectoral response.* 2017.
9. Ramakrishnan, L., *Mycobacterium tuberculosis pathogenicity viewed through the lens of molecular Koch's postulates.* Current opinion in microbiology, 2020. **54**: p. 103-110.
10. Sia, J.K. and J. Rengarajan, *Immunology of Mycobacterium tuberculosis infections.* Microbiology spectrum, 2019. **7**(4): p. 10.1128/microbiolspec. gpp3-0022-2018.
11. Silva, D.R., et al., *Diagnosis of tuberculosis: a consensus statement from the Brazilian Thoracic Association.* Jornal Brasileiro de Pneumologia, 2021. **47**(2):e20210054.
12. Harding, E., *WHO global progress report on tuberculosis elimination.* The Lancet Respiratory Medicine, 2020. **8**(1): p. 19.
13. Behr, M.A., et al., *Latent tuberculosis: two centuries of confusion.* American Journal of Respiratory and Critical Care Medicine, 2021. **204**(2): p. 142-148.
14. Sanchez, A., et al., *Prevalence of pulmonary tuberculosis and comparative evaluation of screening strategies in a Brazilian prison.* The International Journal of Tuberculosis and Lung Disease, 2005. **9**(6): p. 633-639.
15. Techitnutsarut, P. and F. Chamchod, *Modeling bacterial resistance to antibiotics: bacterial conjugation and drug effects.* Advances in Difference Equations, 2021. **2021**(1): p. 290.
16. Llor, C. and L. Bjerrum, *Antimicrobial resistance: risk associated with antibiotic overuse and initiatives to reduce the problem.* Therapeutic advances in drug safety, 2014. **5**(6): p. 229-241.
17. Ventola, C.L., *The antibiotic resistance crisis: part 1: causes and threats.* Pharmacy and therapeutics, 2015. **40**(4): p. 277.

18. Blair, J.M., et al., *Molecular mechanisms of antibiotic resistance.* Nature reviews microbiology, 2015. **13**(1): p. 42-51.
19. Khawbung, J.L., D. Nath, and S. Chakraborty, *Drug resistant Tuberculosis: A review.* Comparative immunology, microbiology and infectious diseases, 2021. **74**: p. 101574.
20. Sommer, M.O., et al., *Prediction of antibiotic resistance: time for a new preclinical paradigm?* Nature Reviews Microbiology, 2017. **15**(11): p. 689-696.
21. Munita, J.M. and C.A. Arias, *Mechanisms of antibiotic resistance.* Virulence mechanisms of bacterial pathogens, 2016: p. 481-511.
22. Arora, G., et al., *Role of post-translational modifications in the acquisition of drug resistance in Mycobacterium tuberculosis.* The FEBS Journal, 2021. **288**(11): p. 3375-3393.
23. Swain, S.S., et al., *Molecular mechanisms of underlying genetic factors and associated mutations for drug resistance in Mycobacterium tuberculosis.* Emerging microbes & infections, 2020. **9**(1): p. 1651-1663.
24. Saderi, L., et al., *Rapid diagnosis of XDR and pre-XDR TB: a systematic review of available tools.* Archivos de bronconeumologia, 2022.
25. Islam, M.M., et al., *Drug resistance mechanisms and novel drug targets for tuberculosis therapy.* Journal of genetics and genomics, 2017. **44**(1): p. 21-37.
26. Gopal, P., et al., *Pharmacological and molecular mechanisms behind the sterilizing activity of pyrazinamide.* Trends in pharmacological sciences, 2019. **40**(12): p. 930-940.
27. Shi, W., et al., *Aspartate decarboxylase (PanD) as a new target of pyrazinamide in Mycobacterium tuberculosis.* Emerging microbes & infections, 2014. **3**(1): p. 1-8.
28. Shi, W., et al., *Pyrazinamide inhibits trans-translation in Mycobacterium tuberculosis.* Science, 2011. **333**(6049): p. 1630-1632.
29. NHS, *Tuberculosis*. 2023 20/05/2023 [cited 2023 04/05]; Available from: https://www.nhs.uk/conditions/tuberculosis-tb/.
30. W.H.O., *WHO consolidated guidelines on tuberculosis. Module 4: treatment-drug-resistant tuberculosis treatment, 2022 update*. 2022: World Health Organization.
31. Turvey, A.K., G.A. Horvath, and A.R. Cavalcanti, *Aminoacyl-tRNA synthetases in human health and disease.* Frontiers in Physiology, 2022. **13**: p. 1029218.
32. Schimmel, P., *The emerging complexity of the tRNA world: mammalian tRNAs beyond protein synthesis.* Nature reviews Molecular cell biology, 2018. **19**(1): p. 45-58.
33. Gomez, M.A.R. and M. Ibba, *Aminoacyl-tRNA synthetases.* Rna, 2020. **26**(8): p. 910-936.
34. Kwon, N.H., P.L. Fox, and S. Kim, *Aminoacyl-tRNA synthetases as therapeutic targets.* Nature reviews Drug discovery, 2019. **18**(8): p. 629-650.
35. Ho, J.M., et al., *Drugging tRNA aminoacylation.* RNA biology, 2018. **15**(4-5): p. 667-677.
36. Tucaliuc, A., et al., *Mupirocin: applications and production.* Biotechnology letters, 2019. **41**: p. 495-502.
37. Jandourek, O., et al., *Synthesis of Novel Pyrazinamide Derivatives Based on 3-Chloropyrazine-2-carboxamide and Their Antimicrobial Evaluation.* Molecules, 2017. **22**(2): p. 223.
38. Lin, J., et al., *Efficient Synthesis and Biological Evaluation of 6-Trifluoroethoxy Functionalized Pteridine Derivatives as EGFR Inhibitors.* Medicinal Chemistry, 2022. **18**(3): p. 353-363.
39. Dlabal, K., et al., *Synthesis and 1 H and 13 C NMR spectra of sulfur derivatives of pyrazine derived from amidation product of 2-chloropyrazine and 6-chloro-2-*

*pyrazinecarbonitrile. Tuberculostatic activity.* Collection of Czechoslovak chemical communications, 1990. **55**(10): p. 2493-2501.
40. Jumper, J., et al., *Highly accurate protein structure prediction with AlphaFold.* Nature, 2021. **596**(7873): p. 583-589.
41. Stumpe, M.C., et al., *Calculation of local water densities in biological systems: a comparison of molecular dynamics simulations and the 3D-RISM-KH molecular theory of solvation.* The journal of physical chemistry B, 2011. **115**(2): p. 319-328.

# THE END